

AD-A037 240

CALIFORNIA UNIV BERKELEY DEPT OF CHEMICAL ENGINEERING
PROPERTIES AND STRUCTURE OF POLYMERIC ALLOYS.(U)
FEB 77 M SHEN, H KAWAI

F/6 7/3

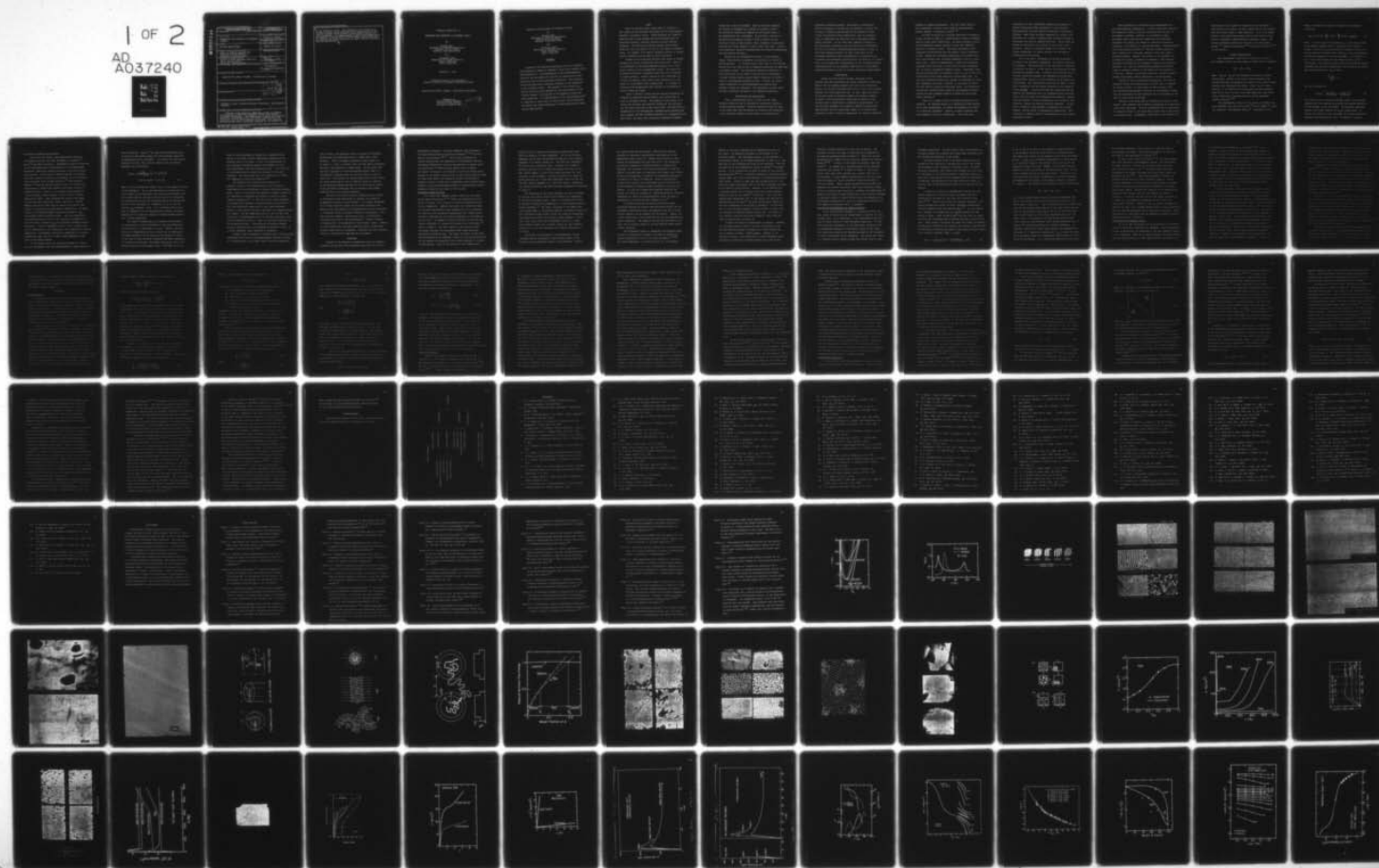
N00014-75-C-0955

UNCLASSIFIED

TR-11

NL

1 OF 2
AD
A037240



ADA037240

SECURITY CLASSIFICATION OF THIS PAGE (When Data Entered)

REPORT DOCUMENTATION PAGE		READ INSTRUCTIONS BEFORE COMPLETING FORM
1. REPORT NUMBER	2. GOVT ACCESSION NO.	3. RECIPIENT'S CATALOG NUMBER
4. TITLE (and Subtitle) Properties and Structure of Polymeric Alloys		5. TYPE OF REPORT & PERIOD COVERED Technical Report
6. AUTHOR(s) M. Shen and H. Kawai		7. PERFORMING ORG. REPORT NUMBER 1417R-11
8. PERFORMING ORGANIZATION NAME AND ADDRESS Dept. of Chemical Engineering University of California Berkeley, California 94720		9. CONTRACT OR GRANT NUMBER(s) N00014-75-C-0955
10. CONTROLLING OFFICE NAME AND ADDRESS Office of Naval Research (Code 472) 800 N. Quincy Street Arlington, Virginia 22217		11. PROGRAM ELEMENT, PROJECT, TASK AREA & WORK UNIT NUMBERS 12. REPORT DATE February 1, 1977
13. MONITORING AGENCY NAME & ADDRESS (if different from Controlling Office)		14. NUMBER OF PAGES 58
15. SECURITY CLASS. (of this report) Unclassified		16. DECLASSIFICATION/DOWNGRADING SCHEDULE
17. DISTRIBUTION STATEMENT (of this Report) Approved for public release: Distribution unlimited		
18. DISTRIBUTION STATEMENT (of the abstract entered in Block 20, if different from Report) DDC RECEIVED MAR 21 1977 A		
19. SUPPLEMENTARY NOTES		
20. KEY WORDS (Continue on reverse side if necessary and identify by block number) Polymeric Alloys; Property-Structure Relations; Multicomponent Polymers.		
21. ABSTRACT (Continue on reverse side if necessary and identify by block number) Because of the generally immiscible nature of polymers, multicomponent polymers or polymeric alloys often exhibit microphase separation. The morphologies of these heterogeneous materials are determined not only by the composition of the system but also by the processing conditions. The resulting microstructures exert a profound influence on the properties		

of the polymeric alloys. The purpose of this review is to discuss the more recent advances in the investigation of the relation between the structure of the polymeric alloys and their properties. An understanding of this relationship would be important in being able to "tailor make" better materials and exploit the unique properties of these materials for engineering applications.

Technical Report No. 11

PROPERTIES AND STRUCTURE OF POLYMERIC ALLOYS

by

Mitchel Shen
Department of Chemical Engineering
University of California
Berkeley, California 94720

and

Hiromichi Kawai
Department of Polymer Chemistry
Kyoto University
Kyoto, Japan 606

February 1, 1977

Technical Report to be published in
American Institute of Chemical Engineers Journal

Approved for public release: Distribution Unlimited

Prepared for
Office of Naval Research
800 North Quincy Street
Arlington, Virginia 22217

EXEMPTION FOR	
DTIC	DATE
DDC	DATE
EXEMPTION	DATE
EXEMPTION	DATE
BY	
DATE	
DATE	
DATE	

Properties and Structure of Polymeric Alloys

by

Mitchel Shen
Department of Chemical Engineering
University of California
Berkeley, California 94720

and

Hiromichi Kawai
Department of Polymer Chemistry
Kyoto University
Kyoto, Japan 606

ABSTRACT

Because of the generally immiscible nature of polymers, multicomponent polymers or polymeric alloys often exhibit microphase separation. The morphologies of these heterogeneous materials are determined not only by the composition of the system but also by the processing conditions. The resulting microstructures exert a profound influence on the properties of the polymeric alloys. The purpose of this review is to discuss the more recent advances in the investigation of the relation between the structure of the polymeric alloys and their properties. An understanding of this relationship would be important in being able to "tailor make" better materials and exploit the unique properties of these materials for engineering applications.

SCOPE

There has recently been a great deal of interest in the studies of the structure and properties of multicomponent polymers or polymeric alloys. These materials are formed by combining two or more polymers by various methods such as mechanical blending, solution casting or direct chemical synthesis. The resulting polymeric systems often exhibit properties that are superior to any of the component polymers alone. For example, high impact resistant plastics or thermoplastic elastomers can be made by these techniques.

Because of the generally positive free energy of mixing, polymers are usually incompatible with each other. Many of the advantages of such multicomponent polymers are in fact direct results of this incompatible nature. By varying the processing conditions, different structures can be obtained in these materials. Recent advances in such techniques as electron microscopy, small angle x-ray scattering etc. now enable us to determine their morphologies. In a number of instances such morphologies bear qualitative resemblance to those in metallic alloys.

Since in metallic alloys new and improved materials are obtained by combining various metals, the analogy here is clear to polymeric alloys. The purpose of this review is to relate the structure and property information now available for the latter materials in the solid state. We begin with an examination of the thermodynamic arguments which explains the basic reasons why that polymers generally are incompatible with each other, and under what constraints compatible polymeric

alloys can in fact be obtained. Next we show some examples of electron micrographs for a series of polymeric alloys. The effects of varying the composition and solvent power on the morphologies are illustrated. Of particular interest is the ability of polymeric alloys to form a regular lattice structure, known as macrolattice, which resembles in appearance the metallic alloys though in a much larger size range. Statistical mechanical theories interpreting the observed morphologies are then briefly discussed.

Because of the heterogeneous nature of most polymeric alloys, their physical properties can sometimes be treated as microcomposites. It is shown that in fact some of the theories dealing with the elasticities of composite materials are applicable to polymeric alloys. The mechanical deformation behavior is then scrutinized in the light of the structural information. A unique "strain-induced plastic-rubber transition" is found to exist in heterogeneous polymeric alloys. Finally, the visco-elastic properties of both homogeneous and heterogeneous polymeric alloys are discussed. The morphology is again shown to exert a profound influence on the observed properties.

CONCLUSIONS AND SIGNIFICANCE

From a technological point of view, new and useful polymeric materials can be obtained by judiciously combining various existing polymers. From the scientific point of view, on the other hand, the correlation of structure and properties of the resulting polymeric alloys poses an interesting and

challenging research problem. The generally incompatible nature of polymers is turned into an advantage if proper care is taken in preparing and processing the polymeric alloys. In fact if molecular mixing takes place, then the polymeric alloy is compatible and there will be no observable morphological features. On the other hand, improper blends will show macroscopic separation and the material will delaminate. The key is to produce microheterogeneous polymeric alloys, so that each component polymer can still retain most of its individual properties while contributes in a synergistic way to provide new macroscopic properties for the material as a whole. Thus, an increased basic understanding of the structure-property relationship will be of paramount importance in tailor-making desirable polymeric alloys for various engineering applications.

INTRODUCTION

During the past several decades, thousands of new polymers have been synthesized by highly sophisticated techniques. Many of the new polymers possess some very novel properties. However, it has been estimated that only 1 or 2% of all of these polymers ever find commercial use. In fact, among the nearly 30 billion pounds of synthetic rubbers and plastic produced annually in the United States, about 80% is based on a few polymers such as polyethylene, polystyrene, polybutadiene, etc. New and novel polymers will always be needed for specialized applications, but for large-scale usage, it is clearly more desirable to find a "winning combination" of existing commercial

polymers to improve performance. For this reason there is now considerable interest in the study of multicomponent polymer systems, or polymeric alloys.¹⁻¹⁹

In order to arrive at a rational definition of polymeric alloys, we show in Table 1 a classification scheme of polymers based on their chain constitution. We define polymeric alloys as multicomponent polymer systems in which the components exists on a polymeric level. Thus block copolymers, graft copolymers and polyblends form the general class of polymeric alloys. Random and alternating copolymers are excluded from this class because their different components exist on a monomeric level. Blends of homopolymers, random and alternating copolymers with each other or with block or graft copolymers are, of course, considered polymeric alloys. Sometimes a more restrictive definition of polymeric alloys is used in the literature which limits these materials to polyblends only. An even more restrictive definition applies to polyblends in which both components are rigid. However, in this paper we prefer the more general definition enunciated above. An interesting quantitative classification scheme of multicomponent polymer systems has been proposed recently by Sperling using group theory concepts.¹²

There are a number of ways in which polyblends can be prepared. The simplest method is to physically blend together two or more homopolymers, or between homopolymers and random or alternating copolymers. However, as shall presently see, most polymeric pairs are incompatible. Block and graft

copolymers are often considered compatibilizing agents to prevent macroscopic phase separation or stratification. Technologically the most important technique is mechanical blending. Most often the major component is a plastic and the minor one a rubber, although quite frequently blends of elastomers are used for rubbery materials. Latex blends are formed by coagulation of a mixture of two or more latex polymers. Finally a convenient method is to dissolve the polymer components in a mutual solvent, and followed by evaporation of the solvent.

All of the above techniques are primarily physical blending of the polymeric components. No chemical reactions are required. The second type of the technique of blending is chemical in nature. In the case of the formation of interpenetrating networks (IPN), a monomer can be imbibed into an existing crosslinked polymer and subsequently polymerized. Alternatively, latexes of linear polymers can be mixed as in latex blends. Now crosslinking agents can be added, so that after coagulation the two polymer networks can be formed by curing in situ. In both instances two crosslinked polymer networks are superposed over, or interpenetrating into each other, hence the name of interpenetrating networks. Another chemical method of forming polyblends is the inverse of IPN formation, namely the solution grafting technique. In this case an existing linear polymer is dissolved in a second monomer, and the latter is subsequently polymerized. This technique is commonly used in the preparation of high impact polystyrene (HIPS).

Most polyblends are microscopically heterogeneous but are macroscopically homogeneous. In other words their structure and composition remain relatively invariant from one part of the sample to another. However, it is possible to make polyblends whose structure and composition are nonuniform throughout the sample, but change as a function of position (gradient) in the sample in a prescribed manner. These materials are called gradient polymers.¹⁹ The most extreme example of such a material is a two-layer laminate, which has a sharp two-step gradient. However, the profile of the gradient can be made to be linear, parabolic or sigmoidal. Both chemical and physical methods can be employed to prepare such gradient polymers. In a way all conventional polyblends are special cases of gradient polymers in the sense that the gradient is a flat one. However, as we shall later see, nonflat gradients produce some rather unusual properties in the polyblends.

Because of their technological importance, the study of polymeric alloys has recently been an active area of research in polymer science. In this paper, we shall present first the interesting morphological features of the polymeric alloys, then the properties of these materials will be discussed in the light of their known structures.

Because of the large body of literature available on this subject, the treatment must therefore necessarily be illustrative rather than exhaustive. Thus our discussions will be restricted to polymeric alloys in the solid state rather than in the molten or solution state. Furthermore, since much of the interest has

been centered on the studies of block and graft copolymers (particularly the former), we shall choose most of the examples from the current works on these materials. It is to be hoped, however, that these restrictions would in fact serve to facilitate a fundamental understanding of polymeric alloys. For further treatments readers are referred to the cited monographs,¹⁻⁵ symposia proceedings⁶⁻¹⁴ and review articles¹⁵⁻¹⁹ on this subject.

POLYMER COMPATIBILITY

The thermodynamic condition for the mixing of two or more systems is that the free energy of mixing must be negative:

$$\Delta G_m = \Delta H_m - T\Delta S_m \quad (1)$$

Where ΔH_m and ΔS_m are the enthalpy and entropy of mixing respectively. Unlike in the case of small molecules, the entropy decreases accompanying the mixing of long chain polymer molecules are generally very small. Since ΔH_m are often positive, it is therefore not surprising that most polymeric pairs do not mix. In fact it has been shown that only under rather exceptional circumstances do we obtain compatible polymer mixtures.^{15,18}

The thermodynamic theory for the mixing of polymers has been developed long time ago by Scott²⁰ and by Tompa²¹, using the classical Flory-Huggins theory.²² According to this

theory, the Gibbs free energy of mixing for two polymers is given by

$$\Delta G_m = RT (v/v_r) \left(\frac{V_A}{x_A} \ln V_A + \frac{V_B}{x_B} \ln V_B + \chi_{AB} V_A V_B \right) \quad (2)$$

where v is the volume of the mixture, v_r is the molar volume of the polymer segment which is considered the reference volume, V 's are the volume fractions of polymers A and B, x 's are the degrees of polymerization and χ_{AB} is the Flory-Huggins interaction parameter for the two polymers. On the basis of eq. 2, the phase diagram for the polymer mixture can be constructed. The spinodal curves, which are boundaries between metastable and unstable compositions, are calculable by setting the second derivative of ΔG_m to zero:

$$\frac{\partial^2 \Delta G_m}{\partial V_A^2} = 0 \quad (3)$$

and can be written as:

$$(\chi_{AB})_{sp} = \left[\frac{1}{2x_A (\bar{V}_A)_{sp}} + \frac{1}{x_B (\bar{V}_B)_{sp}} \right] \quad (4)$$

The binodal curves (boundaries between stable and metastable compositions) are computed by equating the chemical potential of each polymer in the two phases. The resulting equations, however, are rather awkward for actual computations. In general the theory of Scott and Tompa are in good qualitative agreement with experimental data. In specific instances,

qualitative agreement was obtained.

During the last decade, more sophisticated theories of polymers solutions have been developed by Prigogine,²³ Flory²⁴ and their co-workers. Reasonably accurate calculations of the non-combinatorial contributions to the thermodynamic properties, namely the residual functions, have been successfully derived. On the basis of these functions the residual Gibbs free energy of mixing of two polymers can be calculated, which was shown to be strongly positive.²⁵ More recently, McMaster²⁶ used the equation state of Flory in carrying out computations to predict the spinodal and binodal curves for polymer mixtures. Figure 1 is a schematic phase diagram of a binary polymer mixture showing a lower critical solution temperature (LCST). Phase diagrams for mixtures with upper critical solution temperature (UCST) also exist. However, McMaster was able to show from his theory that UCST is less common, in agreement with experimental observations. At small values of the polymer-polymer interaction parameter (χ_{AB}) simultaneous LCST and UCST may exist. They will merge with increasingly positive value of the interaction parameter. On the other hand, a negative χ_{AB} will indicate increasing mutual solubility. Figure 1 emphasizes the fact that a polymer pair may be incompatible at one temperature, but compatible at another temperature. Furthermore, they may be compatible in a certain composition range, but not in other ranges depending on the shape of the phase diagram.

If the polymer pairs are covalently bonded as in block or graft copolymers, then the thermodynamics of phase separation

must be modified. Krause ²⁷ has used the Flory-Huggins model to write the free energy change for the microphase separation of monodisperse block copolymers. By setting the free energy expression to zero, the critical values of the interaction parameter can be evaluated:

$$(\chi_{AB})_{cr} = \frac{zV_r}{(z-2)V_A n_A V_B} \left[- \ln (V_A^{V_A} V_B^{V_B}) + 2(m-1) \Delta S_d / R - \ln (m-1) \right] \quad (5)$$

where z is the coordination number, and m is the number of blocks in the copolymers. ΔS_d is the disorientation entropy which is lost because of the requirement that the junction between the A and B blocks must be located on the surface of the two phases. The theory predicts that the microphase separation becomes more difficult with increasing m . Comparison of eq. 5 with the critical χ_{AB} evaluated from eq. 4 indicates that for the same two polymers with the same molecular weights, the phase separation will occur more readily in simple polymer mixtures than in block copolymers.

The general incompatibility of polymers would prevent the preparation of useful polyblends if the phase separation (stratification) is macroscopic in scale. However, the same feature of incompatibility can be turned into an advantage if the phase separation can be reduced to microscopic in scale. In the case of block and graft copolymers the phase separation is necessarily microscopic (microphase separation) due to the delimiting sizes of the polymer chains. The addition of the

block or graft copolymer to blends has a compatibilizing effect if the block or graft components correspond to the polymers used in the blend. To wit, the incorporation of poly (styrene-g-butadiene) permits the blending of up to 40% polybutadiene (PB) with polystyrene (PS). Only 10% of PB can be blended with PS without the presence of the graft copolymer. The latter thus acts as an emulsifier to render the components in the blend compatible.²⁸

The simplest way to detect phase separation in polymeric alloys is the determination of the transition temperatures by such techniques as dynamic mechanical measurements. Figure 2 illustrates the mechanical damping curves for two copolymers of butadiene and styrene of nearly the same chemical composition.²⁹ In the case of the random copolymer, the damping curve exhibits a single maximum characteristic of the glass transition temperature of the random copolymer. However, in the case of the block copolymer, two damping maxima are evident. The low temperature peak at -80°C is the glass transition of polybutadiene block in the block copolymer, while the high temperature peak at 100°C is the glass transition of the polystyrene block. The existence of multiple damping maxima is characteristic of heterogeneous polymeric alloys, be it block copolymer, graft copolymer or polyblend.

Figure 2 also illustrates a classical case in the principle underlying the utility of microheterogeneous polymeric alloys. It is obvious that in the normal range of service temperature

(say 0°C-40°C), the polymeric alloy of styrene and butadiene possess both the characteristics of a rubber and a glass (plastic). Thus a PS sample containing a small amount of PB (about 5 - 10%) is a plastic that has high impact resistance because of the presence of rubbery phase. On the other hand, the block copolymer of styrene-butadiene-styrene (SBS) is a thermoplastic elastomer when the styrene content is kept to around 30%. The presence of styrene phase acts as both fillers and quasi-crosslinks so that no chemical curing is required. At the meantime rubbery articles can be fabricated by conventional processing techniques such as extrusion and molding normally used in the plastics industry.

The use of the glass transition temperatures as a probe in determining phase separation is, however, not always as unambiguous as Figure 2 might suggest. For example, MacKnight, et.a.³⁰ have found that there are two glass transition temperatures for the polyblend of polystyrene and poly(2,6-dimethyl-1, 4-phenylene oxide) by dynamic mechanical measurements. The same mixtures, however, exhibit only one T_g if differential calorimetry was used in the determination. Another criterion of compatibility is transparency of the mixture in bulk. However, if both polymers have the same refractive index, incompatible polymers would also be transparent. Therefore one must exercise caution in defining the compatibility of polymers.

STRUCTURE

Because of the generally incompatible nature of polymers, polymeric alloys often show microphase separation with various

morphological features. The most frequently used techniques for these observations are electron microscopy³¹⁻⁴⁰ and small angle x-ray scattering.⁴¹⁻⁴³ Since organic polymers all contain carbon atoms, the application of transmission electron microscopy requires the selective introduction of certain atoms for observation.³¹ These staining agents, such as osmium tetroxide or bromine, are believed to react with double bonds. Because of the greater cross section to the electron beam provided by these heavy atoms, the necessary contrast is obtained in polymeric alloys in which one of components contain double bonds. Example of the electron photomicrographs of appropriately stained polymeric alloys will be shown in this section.

Amorphous Polymeric Alloys

For a given two component system, there are five fundamental domain structures.^{44,45} These are schematically illustrated in Figure 3 as a function of relative concentrations of the two components. Lamellar structures are favored by compositions with approximately equal proportions of the components. The spherical and cylindrical morphologies will undergo phase inversion, depending on the relative abundance of one component and the other. An example of these structures is given by the diblock copolymers of isoprene and styrene cast from toluene³⁶ shown in Figure 4. The dark regions in the electron photomicrograph represent the polyisoprene (PIP) phase which was selectively stained by OsO_4 . The domain structure of the 20/80 styrene-isoprene block copolymer (Figure 4a) may be characterized as tiny spheres of polystyrene (PS) blocks dispersed in a matrix of polyisoprene. Those of the 40/60 and 50/50 compositions

(Figure 4b and 4c) appear as alternating stipes which would really be lamellar in three dimensions. For the 40/60 block copolymer, we now have the cylindrical domains of the isoprene component in PS matrix (Figure 4d). The dark dots represents the ends of the cylindrical rods. In Figure 4e is shown an ultrathin section cut in a different lateral direction of the same (40/60) sample, in which the stripes represent the long direction of the cylinders. Finally in Figure 4f is shown the domain structure of a 70/30 block copolymer, which now has the dark (PI) spheres embedded in a light (PS) matrix. Comparison with Figure 4a verifies the phase inversion phenomenon illustrated in Figure 3.

The morphology of the block copolymer can also be changed by changing the casting solvent while keeping the composition of the block copolymer fixed. Figure 5 illustrates the effect of various solvents on the morphology of a 40/60 styrene/isoprene diblock copolymer.³⁶ The domain structure of the sample cast from toluene shows an alternating lamellar arrangement (Figure 5a). That from methyl ethyl ketone (Figure 5b) exhibits considerable interconnections between the styrene (light) domains. On the other hand, those cast from cyclohexane (Figure 5c), carbon tetrachloride (Figure 5d), n-hexane (Figure 5e) and n-heptane (Figure 5f) all can be classified as PS domains dispersed in PI matrix.

The effect of the solvent on the morphology of block copolymers may be attributed to the solvation power of the solvents for the respective blocks in the copolymer. Toluene

is a good solvent for both blocks, therefore the lamellar structure is observed as predicted by consideration of the composition alone (Figure 3). Methyl ethyl ketone is a good solvent for polystyrene but a poor one for PI, the morphology may thus be regarded as a mixed structure of lamellae and dispersed (PI) cylinders in PS matrix. Cyclohexane is just the reverse in solvent power in comparison with methyl ethyl ketone, so the mixed morphology of lamellar and dispersed polystyrene cylinders in PI matrix is observed. Carbon tetrachloride, n-hexane and n-heptane are increasingly poor solvents for PS, so the dispersed PS domains become increasingly irregular and smaller. In fact the n-hexane and n-heptane solutions are cloudy, and should be regarded as pseudo-solutions or colloidal suspensions in which the precipitated PS chains are kept in suspension by the solvated block segments of PI.³⁶

It should be pointed out that the different domain structures obtained by casting from different solvents are not necessarily equilibrated ones, but apparent ones due to interactions between A and B segments and the solvent. Indeed, for a given composition, there should be only one thermodynamically stable morphology. The apparent non-equilibrated domain structures can be readily changed to the equilibrated ones by proper thermal annealing.

The progressive change in morphology with changing compositions as illustrated in Figure 3 can also be achieved by adding homopolymers A or B to the block copolymer.^{41,43-50} The added homopolymer is solubilized into the corresponding

domains in the block copolymer by the emulsifying action of the latter. An important parameter in such blends is the molecular weight. The emulsifying action is only possible if the molecular weight of the added homopolymer is equal to or less than that of the corresponding block in the copolymer. This can be predicted by the thermodynamic theory of Krause²⁷ discussed earlier. As in illustration, we show in Figure 6a the electron photomicrograph^{48,50} of a triblock copolymer of styrene-butadiene-styrene (SBS) cast from a mixed solvent of tetrahydrofuran/methyl ethyl ketone. Figure 6b shows that the incorporation of a low molecular weight polystyrene (PS) in the block copolymer enlarged the PS domains (light regions). However, if the added PS has a molecular weight that is greater than that in SBS, separate domains of pure PS are formed⁵⁰ (Figure 6c). Now if we add polybutadiene homopolymer (PB) to the system, the same type of observations can be made.⁴⁸ By using low molecular weight PB, the basic morphology of the system is preserved. On the other hand, if the molecular weight of the PB is high, we again find the formation of separate domains (Figure 6d). Of course in this instance these are the dark PB domains, rather than the light PS domains seen in Figure 6c.

Although the essential morphologies of spheres, lamellae and cylinders shown in Figure 3 are well illustrated by the electron photomicrographs in Figures 4-6, these features are not as regular as Figure 3 might suggest. However, it is possible to observe long range order in block copolymers under appropriate conditions of specimen preparation, such as melt

extrusion, thermal annealing or slow rate of casting. The existence of such long range of order was first suggested by the electron photomicrograph of Fisher.⁵¹ These are now well documented for a number of block and graft polymers by numerous workers.⁵²⁻⁵⁹ A review of this topic has recently been published.⁶⁰ An example for a styrene-butadiene block copolymer containing 68% styrene⁵² is shown in Figure 7. The nearly perfect long range order extends over a rather large area of the specimen. In some samples imperfections in the long range order may appear as "grain boundaries" normally observed in metallic systems. These electron photomicroscopic studies are supported by evidence from small angle x-ray scattering (SAXS) as well as optical light scattering. McIntyre and Compoz-Lopez⁵⁵ showed on the basis of SAXS results that an SBS triblock copolymer of molecular weights 21,100/63,400/21,100 can be assigned to an orthorhombic macrolattice of unit cell dimensions 676/676/566 Å with spherical PS domains 356 Å in diameter.

Statistical Thermodynamics of Domain Formation

As we have already discussed in a previous section, the free energy of mixing for two homopolymers is positive for most polymer pairs. As a consequence, it is thermodynamically favorable for such mixtures to show macrophase separation. For the block and graft copolymers, on the other hand, different kinds of incompatible polymers are covalently linked to each other. This restriction prevents the demixing process of the copolymers to lead to macroscopic phase separation. The system must remain at a certain positive though minimum free energy level to show

microphase separation. The free energy level is determined by a balance between the enthalpy and energy terms consistent with the equilibrium morphology of the system.

The basic driving force of the phase separation may be ascribed to the reduction in the positive surface free energy of the system by the increase of the domain size. For block and graft copolymers, this domain size increase will give rise to a decrease in the volume fraction of interfacial region in which the junction points of the copolymers must be distributed. In addition, configurations of the sub-chains must change in order to even up the density deficiency in the interior of the domains.

A number of statistical thermodynamic theories for the domains formation in block and graft copolymers have been formulated on the basis of this idea, but differing in details.⁶¹⁻⁶⁸ Figure 8 and 9 show the schematic diagrams of the domain formation for block and graft copolymers respectively. The most pioneering work was done by Meier.⁶¹ In his original work, however, he assumed that the boundary between the two phases is sharp. Leary and Williams⁶² were the first to recognize that the interphase must be diffuse and has a finite thickness. These authors calculated the Gibbs free energy of demixing by separately estimating the enthalpic and entropic contributions. The enthalpy of demixing was based on the regular solution theory. For a triblock copolymer (ABA), it reads

$$\Delta H_m = -v_m V_A V_B (\delta_A - \delta_B)^2 + f v_m \overline{V_A V_B} (\delta_A - \delta_B)^2 \quad (6)$$

In eq. 6, the first term is the enthalpy of complete demixing of the polymers, while the second term is a correction term that takes into account of the presence of the mixed interphase region. δ_A and δ_B are solubility parameters of A and B blocks. v_m is the molar volume of the mixture, and V_A and V_B are the respective volume fractions. $\overline{V'_A V'_B}$ is the volume averaged product of A and B fractions in the mixed region, and f is the overall volume fraction of the mixed region. Values of f are calculated from the overall composition of the block copolymer, and depends on the geometry of the domain (spheres, cylinders or lamellar). The entropic term consists of three contributions:

$$\Delta S_m = \Delta S_1 + \Delta S_A + \Delta S_B \quad (7)$$

ΔS_1 is the entropy change resulting from the requirement that one of the junctions of the A-B blocks must be placed in the mixed region (Figure 10). ΔS_A is associated with the stipulation that one end of the A-chain must be in the mixed region and the other in the A-region; while ΔS_B is due to the fact that both ends of the B-chain in the triblock copolymer must be in the mixed region. By minimizing the free energy obtained from these respective contributions, Leary and Williams were able to predict the favored morphology for triblock copolymers. In addition, based on this model these authors also suggested the existence of a "separation temperature", T_s , at which the micro-phase separated system and a homogeneous mixed system of A and B would be equilibrium. T_s is obtained by setting the free energy

of the block copolymer to zero, thus it is just the ratio of the enthalpy to entropy. The prediction seems to be consistent with some of the experimental findings.^{69,70}

The more recent papers by Helfand^{67,68} used very elegant mean field approach to inhomogeneous systems. His predictions of domain sizes as a function of molecular weight agree well with the data of Douy, et.al.⁷¹ The calculated interfacial thicknesses also compare favorably with recent SAXS results by Hashimoto, et.al.^{43,72} Kawai and coworkers⁶⁴ treated the problem from the point of view of micelle formation. As the solvent evaporates, a critical micelle concentration is reached, at which the domains are formed and are assumed not to change upon further drying. Minimum free energies for an AB-type block copolymer were computed this way, the results are shown in Figure 11. It can be seen here that at low weight fractions of A (below V_1), the spherical morphology has the lowest free energy and is favored. Between V_1 and V_2 , rods or cylinders are expected to form. As V_1 becomes greater than V_2 (nearly equimolar) then the lamellar morphology is the equilibrium structure. These predictions are consistent with the schematic diagrams of domain morphologies given in Figure 3.

Semicrystalline Polymeric Alloys

So far we have discussed only the morphologies of polymeric alloys in which both components are amorphous. Here the dominant factor in determining the morphology is the free energy of mixing of the components. When one of these components is crystallizable, then the crystallization of this component will also play a role

in determining the morphology of the system.⁷³⁻⁸¹ As an example, we show in Figure 12 the cross-polarized photomicrographs of benzene-cast specimens of poly(ethylene oxide), or PEO, and triblock copolymers of ethylene oxide-isoprene-ethylene oxide (EO/IP/EO) of various compositions.⁷⁹ For the pure PEO, which is crystalline, the well-formed spherulites are clearly seen in Figure 12a. With increasing fraction of the amorphous polyisoprene (PIP) components, the texture with negative birefringence becomes less perfect, leading to more blurred Maltese-cross patterns. Since the spherulites impinge upon each other, the implication is that most of the block segments must be located within the spherulites.

The fine structure of the same block copolymers can be elucidated by transmission electron microscopy.⁷⁹ The micrograph for the block copolymer containing 75% ethylene oxide (Figure 13a) shows dark spherical domains of approximately 0.1 μm in diameter are dispersed in the light matrix. The dark regions are the polyisoprene domains stained by OsO_4 , while the light domains belong to the crystalline, unstained PEO. The texture of the PEO matrix is seen to be spherulitic in the shadowed specimen (Figure 13b). As the fraction of PIP increases, the spherical dark domains become more interconnected, resulting in the structure of cylinder-like PIP domains dispersed in spherulitic PEO matrix (Figure 10c). With further increase of the PIP fraction (48%), the dark phase becomes continuous (Figure d). However, the PEO phase is still spherulitic, as seen in Figure 13d, though somewhat disordered. Finally, in

in Figures 13e (86% PIP) and 13f (91% PIP), a phase inversion occurs at very high PIP content. Spherical PEO domains having average diameter of approximately 400 \AA are dispersed in the PIP matrix. Wide angle x-ray diffraction studies show that these PEO domains are still crystalline.

A hypothetical molecular structure of crystalline block copolymer⁷⁹ is shown in Figure 14. Here it is demonstrated that the individual crystallites of the crystallizable component can form spherulites as in homopolymers, the amorphous components are rejected out of the crystallites and reside in the inter-crystalline phase. This structure is seen to be composed of the folded-chain crystals. An alternative model for segmented block copolymers consisting of the fringed-micelle crystalline regions has been proposed by Wilkes.⁸⁰

The nature of the casting solvent also plays an important role in determining the morphology of semicrystalline polymeric alloys. For EO/IP/EO systems, the same polymer cast from ethyl benzene will give single crystal-like texture.⁷⁹ In the case of a segmented copolyester consisting of poly(tetramethylene ether glycol terephthalate) (PTMEGT) and sequences of tetramethylene terephthalate (4GT), casting from 1,1, 2-trichloroethane results in a spherulitic structure, while the same polymer cast from tetrachloroethane does not.⁷⁷

The sizes of the spherulites in block copolymers appear to depend on the content of the crystallizable segments. The replica electron micrographs⁷⁷ for the copolyester of PTMEGT and 4GT are shown in Figure 15. As the 4GT content increases

from 54 to 81 wt %, the spherulites sizes increase from about 1 μm to nearly 10 μm . The trend is confirmed by light scattering experiments on the same samples. Similar observations have also been made in other systems.⁸⁰

PROPERTIES

Elastic Moduli

Since most of the polymeric alloys are heterogeneous in nature, they may be considered as a class of composite materials. However, the dispersed phase in the polymeric alloys are microscopic in dimensions, in contradistinction to "ordinary" composite materials such as fiberglass in which the dispersed fibers are macroscopic in dimension. Nevertheless a number of existing theories for the elasticity of composites can be applied to polymeric alloys, with notable success.

Among the first who treated the elastic moduli as composites were Takayanagi⁸² and Kawai⁸³ and their coworkers. Figure 16a indicates that a given composite (right hand side) may be represented by an equivalent model (left hand side) depending on the degree of mixing (λ) of the dispersoids and the composition (ϕ) of the dispersoids and matrix. Perfect adhesion between the phases is assumed. When the equivalent model is stretched, the resulting stress may be borne by the matrix alone or by both the matrix and the dispersed phases. The modulus of the equivalent model can be calculated by two possible mechanical models. They are the (I) Series Model and (II) Parallel Model, shown in Figure 16b. For the Series Model, the modulus M (dynamic or

transient; shear, tensile or bulk) of the composite is

$$M = \lambda \left[\frac{\phi}{M_d} + \frac{(1-\phi)}{M_m} \right]^{-1} + (1-\lambda) M_m \quad (8)$$

and for the Parallel Model, it becomes

$$M = \left[\frac{\phi'}{\lambda' M_d + (1-\lambda') M_m} + \frac{(1-\phi')}{M_m} \right]^{-1} \quad (9)$$

where subscripts d and m refer to dispersed and matrix phases respectively, V's are the volume fractions of the two phases, and $\lambda\phi = V_d$. The unprimed λ and ϕ refer to the Series Model, while the primed ones to Parallel Model. The two models are in fact equivalent, as shown by Dickie⁸⁵ and by Kaplan and Tschoegl⁸⁶, if $\lambda' = 1 - V_d - \phi$. Eqs. 8 and 9 have been employed by a number of authors⁸¹⁻⁸⁸ to compare with experimentally determined elastic moduli of polyblends and block copolymers. However, because of the essential equivalence of these two models, the interpretation of their physical significance becomes difficult.

A theory for a composite in which spherical dispersoids are embedded in a matrix has been developed by Kerner⁸⁹ for the shear moduli and bulk moduli. Later Christensen⁹⁰ also derived the complex moduli for the same model. Their final results are identical and can be represented by

$$\frac{M}{M_m} = \frac{(1-V_d)M_m + (\alpha V_d)M_d}{(1+\alpha V_d)M_m + \alpha(1-V_d)M_d} \quad (10)$$

where ν_m is the Poisson ratio of the matrix and

$$\alpha = 2(4-5\nu_m)/(7-5\nu_m) \quad (11)$$

In arriving at eq. 10, the following assumptions were made:

- (1) Inter-particle interactions are negligible;
- (2) Matrix-dispersoid adhesion is perfect;
- (3) The Poisson's ratio is a real constant;
- (4) There is a random distribution of dispersoid; and
- (5) Properties of the constituent phases are the same as their properties in bulk.

Assumptions 1 and 2 are generally considered less drastic than 3 and 4. The validity of assumption 5 is somewhat difficult to assess at this time. However, despite these assumptions, the model has been found to be satisfactory in correlating experimental data.⁸⁵⁻⁸⁷

Both the Takayanagi-Kawai theory and the Kerner-Christensen theory are valid for soft dispersoids in hard matrix. It has been found that the inverse case of hard dispersoids in soft matrix cannot be adequately represented by these models. Halpin and Tsai^{91,92} have provided a general derivation for an equation that covers the complete range of moduli. The equation, modified by Nielsen^{93,94} for hard dispersoids in soft matrix is:

$$\frac{M}{M_m} = \frac{1 + AB V_d}{1 - B\psi V_d} \quad (12)$$

where

$$B = \frac{M_d/M_m - 1}{M_d/M_m + A} \quad (13)$$

$$A = k - 1 \quad (14)$$

$$\psi = 1 + (1 - V_d^*) V_d / V_d^* \quad (15)$$

k is a generalized Einstein coefficient, and ψ is a function that accounts for the maximum packing fraction, V_d^* is related indirectly to morphology and usually $0.5 < V_d^* < 0.9$. For inverted composites in which the matrix is hard, then

$$\frac{M_m}{M} = \frac{1 + A' B' V_d}{1 - B' \psi V_d} \quad (16)$$

when

$$B' = \frac{M_m/M_d - 1}{M_m/M_d + A'} \quad (17)$$

$$A' = 1/A$$

The primes in eqs. 16-18 refer to the inverted system. The advantage of Halpin-Nielsen theory is that it can take into account the morphology of the two-phase system. The Einstein coefficient is particularly sensitive to the morphology, and a list of its values is available for a number of different morphologies.⁹⁴ Thus in principle if the morphology of a polymeric alloy is known, then the moduli can be calculated by either eq. 12 or eq. 16.

We have already shown previously that as the composition of the polymeric alloy changes a phase inversion may occur at a certain point. For such a situation, Nielsen has proposed the following mixing rules:

$$\log M = V_U \log M_U + V_L \log M_L \quad (19)$$

where M_U and M_L are the upper and lower bounds to the modulus at a given composition, and V_U and V_L are the fractions of high and low modulus materials in the overlap region where both phases are continuous (neither are dispersoids). For any given overall composition V ,

$$V_L = \frac{V - (1-V_d^*)}{V_d^* - (1-V_d^*)} \quad (20)$$

$$V_U = 1 - V_L = \frac{V_d^* - V}{V_d^* - (1-V_d^*)} \quad (21)$$

Figure 17 shows the tensile modulus data for an SBS triblock copolymer. The theoretical curve that produced the best fit to the data yielded the following values: $A = 3.0$, $V_d^* = 0.8$ for PS dispersed in PB matrix, and $A' = 0.86$, $V_d^* = 0.85$ for the inverted case. These values suggest that at low PS concentrations, the PS domains are either aggregates of about 6 spheres or rods with an aspect ratio of 6 - 10. Both PS and PB phases tend to be continuous in the range of 15 - 80% PS. Above 80%, PB domains are dispersed in PS matrix as spheres. These findings are in general agreement with the electron microscopic observations discussed in the previous section.

Tensile Properties

Many of the polymeric alloys now in commercial use are consisted of a soft rubbery component and a hard glassy or semicrystalline component at a given service temperature.⁹⁵⁻⁹⁹

The tensile properties reflect the composition of the polymeric alloys.⁹⁸⁻¹⁰³ Figure 18 shows the stress-strain behavior

of a series of triblock copolymers of styrene-butadiene-styrene.⁹⁸ At high butadiene content, the material can be stretched to nearly 1,000 % strain. This behavior is of course characteristic of the high extensibility of rubbers. As the styrene content increases, the stresses are higher at comparable strains due to the filler and crosslinking effects of the plastic domains. At 39% styrene, it becomes possible for the plastic domains to form inter-connectivities, thus there is some evidence of drawing at the low strain regions, while the high extensibility is retained. As styrene content becomes dominant, there is now more drawing and lower extensibility (more plastic-like). At 80% styrene, the SBS undergoes yielding and fractures at low strains.

The relation between the tensile behavior and the morphology of the polymeric alloys is very illuminating. Kawai and coworkers¹⁰⁴ have shown that for a 50/50 diblock copolymer of styrene-isoprene cast from a mixed solvent system of toluene and methyl ethyl ketone, one observes yielding and drawing in the stress-strain curve (Figure 19). The transmission electron micrographs in Figure 20 show that outside of the region where the drawing occurs (20a), the structure of spherical rubber domains are essentially unaffected. At the boundary of the drawn region, there is evidence of the elongation of the spheres (20b). The deformation becomes extensive in the region of drawing (20c). At the outer skin layer of this region where the strain is highest, the domain structures are destroyed (20d). The authors attributed the latter morphological changes to the

heat transformed from the strain energy, which caused the flow to take place upon stretching.

Under appropriate conditions of sample preparation, the phenomenon of "strain induced plastic-rubber transition" can be observed.¹⁰⁵ It is known that for block copolymers and polyblends, there is a yielding and drawing region in the first stress-strain cycle. However, in second and subsequent deformations the material exhibits considerable strain-softening.⁹⁹⁻¹⁰¹ Figure 21 shows the stress-strain curves of SBS and SBS blended with a homopolymer of styrene at various weight fractions and cast from a mixed solvent of tetrahydrofuran and methyl ethyl ketone. There is a definite yielding and drawing behavior for all but the sample containing 80% PS which showed macrophase separation. In these cases, the drawing process occurs with the narrowing of the cross-sectional area of the sample suddenly appearing at one point in the sample, which then grows continuously until the entire sample is covered. Such phenomena are similar to that in conventional plastics, except that in this instance the necked regions is no longer plastic but rubbery. After the necking process has propagated throughout, the sample which was initially plastic now is completely rubbery. After the transformation is complete, subsequent stress-strain curves resemble that of a rubber (Figure 22). The electron micrographs in Figure 23 show that there is extensive disruption of the continuous polystyrene domains,¹⁰⁶ which may have been the underlying mechanism of this "plastic-rubber transition". If the sample is allowed to rest for several days, or annealed at elevated temperature, then a "healing effect" is observed whereby the sample

returns to the plastic state.

In the industrial processing of polymers, e.g., extrusion, molding, etc., the material is often subjected to flows in the molten state and followed by rapid cooling. Because of the inherent microstructure in polymeric alloys, anisotropy can often be introduced by such processing operations.¹⁰⁷ Figure 24 shows the tensile behavior of the SBS block copolymer. For the sample that has undergone shearing at high temperatures, the stress-strain curves are quite different for the sample cut normal or parallel to the shearing directions. The anisotropic structure was confirmed by small angle x-ray scattering data. The interpretation is that melt-shearing deformed the spherical domains in the direction of flow. The elongated domains in the longitudinal direction can more easily merge with each other to result in increased continuity of the polystyrene domains, whereas the same ellipsoids will have fewer connectivities in the transverse direction. This is in agreement with the observed tensile data in that the longitudinal sample in fact exhibits higher stress at comparable strains than the transverse ones.

The mechanical properties of a macrolattice of SBS has been investigated.^{108,109} Folkes and Keller¹⁰⁸ used a sample which is consisted of a hexagonal array of polystyrene cylinders embedded in the polybutadiene matrix. The diameter of the cylinders is of the order of 15 nm, and the hexagonal lattice parameter is 30 nm. As shown in Figure 25, the stress-strain curves of the macrolattice show a decisive anisotropy. The authors calculated the moduli by a simple Takanayanagi-Kawai

model, and found excellent agreement if the longitudinal sample is represented by parallel coupling and the transverse sample by series coupling.

Another class of anisotropic polymeric alloy is the gradient polymer.¹¹⁰ One method of forming a gradient polymer is to allow a monomer to diffuse into a sheet of a crosslinked polymer which is in the glassy state. The diffusion rate is low in glassy polymers. Thus when the polymer is removed from the monomer bath before an equilibrium swelling is reached, there is a concentration profile of the monomer in the polymer. This profile can be "fixed" by quickly polymerizing the guest monomer in the host polymer, and the result is a gradient polymer. Of course if the diffusion is permitted to take place for a longer time until an equilibrium concentration of monomer is established throughout the host polymer, then an interpenetrating network (IPN) is formed. Figure 26 shows that pure poly(methyl methacrylate) will undergo brittle fracture at low strains. When a gradient polymer was formed by diffusing methyl acrylate into the poly(methyl methacrylate), the fracture strain is increased with increasing concentration of methyl acrylate. The same results, however, are not achieved when an IPN is formed with the same composition (Figure 27). It is believed that the gradient structure may have enabled the polymer to redistribute the stresses so that yielding can occur before the stresses exceed the elastic limit to undergo fracture.

Viscoelastic Properties

It is now well known that polymeric materials in general exhibit time-dependent mechanical properties. These materials

are considered viscoelastic in nature. The viscoelastic behavior of the polymeric alloys is, however, also very different depending on whether they are homogeneous or heterogeneous. For example, we have mentioned earlier that given the same chemical composition, some polymeric alloys may be homogeneous and some may be not. In Figure 28 we compare the dynamic mechanical data for a poly(α -methyl styrene-*b*-styrene-*b*- α -methyl styrene) with a polyblend of polystyrene and poly(α -methyl styrene).¹¹¹ The latter was prepared by precipitation in methanol of a common benzene solution of the two homopolymers. It is obvious that for the polyblend, there are two distinct transitions at 115°C and 183°C which are the glass transition temperatures respectively of PS and P α MS. The presence of multiple loss peaks, of course, signifies the presence of phase separation. The block copolymer, on the other hand, shows only one glass transition peak at the intermediate temperature, and is therefore considered homogeneous.

A very useful technique in the study of viscoelasticity of polymers is the Time Temperature Superposition Principle.¹¹²⁻¹¹⁴ On the basis of this Principle, it is possible to shift the modulus-time isotherms at a series of temperatures into one single master curve. The shift (a_T) data must follow the Williams-Landel-Ferry (WLF) equation.¹¹⁵ The validity of this technique has been amply demonstrated for a large number of homogeneous polymers.¹¹²⁻¹¹⁴ It has been found that similar data for S- α MS-S block copolymers^{116,117} can be shifted into meaningful master curves. An example is shown in Figure 29. In addition, Figure 30 shows that the shift factor data follow

the WLF equation very well. Thus we have an additional evidence to verify the homogeneous nature of this block copolymer system.

Since the viscoelastic behavior of homogeneous polymeric alloys is similar to that of the conventional homopolymers, it would be of interest to examine the molecular dynamics of these polymeric alloys in the light of the theories developed for homopolymers. The most accepted model^{113-115,118} is that developed by Rouse¹¹⁹, Bueche¹²⁰ and Zimm¹²¹. The RBZ model divides the polymer molecule into $N + 1$ submolecules (beads) held together with N springs. The springs are stretched when the polymer coil is disturbed by a shear gradient. The spring constant is given by $3kT^3/b^2$, where b^2 is the average end-to-end distance of the submolecule. The preceding expression is obtained by taking the submolecule as a random chain which follows Gaussian statistics. As the beads move through the medium, a viscous drag is exerted on them whose magnitude is given by a friction coefficient f . At the cessation of flow, the viscous and elastic forces are equal to each other. Thus the equation of motion can be written, in simplified form, as follows:

$$\dot{\underline{x}} = \sigma \underline{Z} \underline{x} \quad (22)$$

where \underline{x} and $\dot{\underline{x}}$ are column vector of bead positions and bead velocities, \underline{Z} is the nearest neighbor matrix and $\sigma = 3kT/b^2 f$.

In the case of block copolymers,¹²² the above equation must be modified to take into account the fact that not all the beads are the same (as is the case for homopolymers). For

alloys are in fact heterogeneous, their viscoelastic behavior is expected to be quite different.¹²⁹⁻¹⁴⁹ In Figure 32 is shown the modulus-time isotherms for a sample of SBS cast from a mixed solvent system of 90% tetrahydrofuran and 10% methyl ethyl ketone.¹⁴⁴ If these isotherms are now shifted according to the simple Time Temperature Superposition Principle, it is possible to obtain a viscoelastic master curve shown in Figure 33. The reference temperature for this master curve is 25°C. One of normal methods of checking the validity of the Superposition Principle is to perform separate long term experiments as well as high frequency (short time) experiments to compare with the master curve. In Figure 33, the closed circles are data from the former experiments.¹⁴⁴ The open circle is that obtained by acoustic spectrometer at kilocycle frequencies. Both sets of data appear to agree with the master curve quite well.

However, it is important to recall that the basic tenet of the Time Temperature Superposition Principle is valid only if all of the relaxation mechanisms are affected by temperature in the same manner.¹¹²⁻¹¹⁴ Materials obeying this Principle are said to be thermorheologically simple. In other words, relaxation times at one temperature T are related to the corresponding relaxation times at a reference temperature T_r by a constant ratio a_T :

$$a_T = \tau_i(T) / \tau_i(T_r) \quad (25)$$

For heterogeneous systems, the constituent polymers exist in

separate phases and must undergo relaxation processes individually. Such heterogeneous polymeric alloys must therefore in general not satisfy the stipulation given by eq. 25, and should in most instances be thermorheologically complex.

One anomaly is the shift factor data used in constructing the master curve, as shown in Figure 34. They are clearly different from the shift factor data for the homogeneous block copolymers (Figure 30). Only a portion of this curve can be described by the WLF equation, which is related to the relaxations of the polybutadiene phase. The other straight line portion can be fitted to the modified WLF equation of Rusch¹³⁰ which is valid for relaxation of the glassy region (in our case the polystyrene domains). Other type of interpretations for the shift factor have also been advanced by various workers.^{132,137,145} That more than one WLF equation is needed for the shift factor data is an indication of the thermorheological complexity of the heterogeneous materials. Fesko and Tschoegl^{135,145} decomposed the shift factor of a heterogeneous block copolymer as follows:

$$\log a_T = n_A \log a_{TA} + n_B \log a_{TB} \quad (26)$$

where n_A and n_B are the weighting factors. A schematic diagram of the weighting factors as a function of temperature is given in Figure 35. The relatively sharp transition from one dominating relaxation to another at a given temperature reflects the fact that shift factor data in different temperature regions can be explained by different types of WLF equations (Figure 34).

In addition, the excellent agreement between the master curve and experimental data in the long-time end, where only one relaxation mechanism is dominating (Figure 33), is also a consequence of this sharp transition. However, there is at this time no a priori method to determine the weighting factor illustrated in Figure 35. Thus it is necessary to emphasize this fact by the broken mid-section of the master curve in Figure 33.

Another way to understand the thermorheological complexity of the heterogeneous polymeric alloys is shown in Figure 36. Here we see that the master curves for a given polymeric alloy are in fact different in shape at different temperatures, because the relaxation times of the two different phases are affected by temperature differently. However, the experimentally accessible range (which may be called "the experimental window"¹³⁵) is small. Thus within this window the neighboring isotherms appear to be superposable by simple horizontal shifting along the logarithmic time axis. However, the result of such shifting would give reason to an erroneous master curve. This "forced" shifting is the reason that the master curve in Figure 33 is unrealistically wide. It spans more than three logarithmic decades of time, which is twice the time scale covered by the homogeneous block copolymer (Figure 29).

The thermorheological complexity of a heterogeneous block copolymer has been demonstrated by Shen, et.al.¹⁴³ The master curve was determined by stress relaxation methods in the time interval of $10^2 - 10^5$ seconds. By using the well known inter-

conversion techniques,¹¹²⁻¹¹⁴ the master curve can be converted into loss tangent data. Then using the empirical shift factors (Figure 34), the loss tangent are expressed as a function of temperature. Now by using the ultrasonic technique at 9 megahertz, loss tangent of the same sample was determined over the same temperature range. If the block copolymer were thermorheologically simple, the two curves should superpose as demonstrated previously for homopolymers. Figure 36 shows that these two curves in fact are quite different in their temperature positions. Thus the thermorheological complexity of this material is established.

The effect of morphology on the viscoelasticity of block copolymers has been investigated.^{133,140} The most important factor to be considered is the connectivity of the domains. For instance, if the sample was cast from a solvent which results in extensive interconnections among the hard domains (for instance the glassy PS domains in SBS), then the modulus in the regions between the glass-rubber transition of PB and the flow region (above the T_g of PS) will be relatively high. On the other hand, if the hard domains are dispersed in a soft matrix (the rubbery PB domains), then the moduli in the same region will be lower for the same sample.¹³³ Also, the ratio of storage moduli (E'/G') in tensile and shear modes was found to be nearly three for the PB-continuous SBS. This is the expected ratio for elastomers. However, the same ratio for the same sample which was cast from solvents that render them PS-continuous becomes more than 30. The anomalously high value is attributed to the PS domain connectivity.¹⁴⁰

Recently, Kraus and Rollman¹⁴⁹ reported the dynamic viscoelastic properties of SBS which appears to be in support of the diffuse interphase model of the statistical theory.^{62,65,67,68} A series of block copolymers were synthesized which have the identical chemical composition, but differ in block lengths. It was found that the effect of shortening the block length was to decrease the glass transition loss peak of the PS domains. The interpretation is that the size of the interphase domain increases with decreasing block lengths, implying that the composition of the interphase is asymmetric and PS-rich. Kraus and Rollman constructed a model in which the "purity" of the phases decreases with the decreasing block length, and conducted that the existence of a mixed interphase layer does not necessitate the appearance of a third loss peak between the primary transitions of the pure blocks. The model is in satisfactory qualitative agreement with experimental observations.

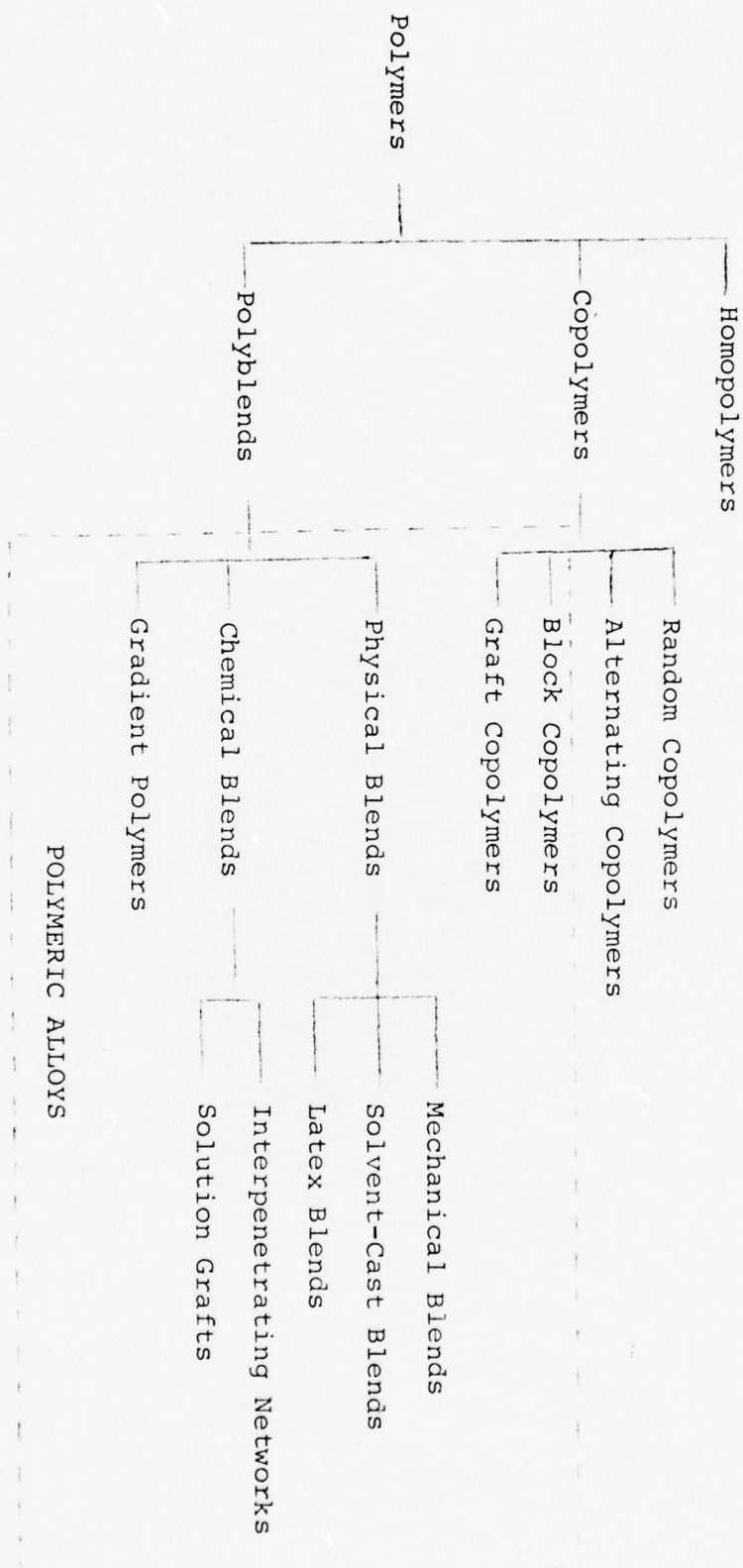
The viscoelastic behavior of triblock and multiblock copolymers blended with homopolymers and diblock copolymers has been studied by a number of workers.¹⁴⁹⁻¹⁵³ Generally the mechanical relaxations can be readily attributable to those of the components. The most interesting observations is the presence of entanglement relaxations in these polyblends. Triblock copolymers, with both end blocks anchored in the hard domains, usually show no entanglement slippage. Upon addition of the homopolymers or diblock copolymers, such slippage now becomes possible. An example of such viscoelastic relaxations is shown in Figure 37. A mathematical model for such entangle-

ment slippage has been proposed by Cohen and Tschoegl¹⁵⁰ for the case of triblock-diblock blends, which was found to be in good agreement with experiments.

ACKNOWLEDGEMENT

This work was supported by the Office of Naval Research, and by the Japan Society for the Promotion of Science.

Table 1. Classification of Polymers on the
Basis of Chain Constitution



REFERENCES

1. W. J. Burlant and A. S. Hoffman, "Block and Graft Polymers", Reinhold, New York, 1960.
2. R. J. Ceresa, "Block and Graft Copolymers", Butterworth, London, 1962.
3. H. A. J. Battaerd and W. G. W. Tregear, "Graft Copolymers" Interscience, New York, 1967.
4. J. A. Manson and L. H. Sperling, "Polymer Blends and Composites", Plenum, New York, 1976.
5. A. Noshay and J. E. McGrath, "Block Copolymers: Overview and Critical Survey", Academic Press, New York, 1976.
6. J. Moacanin, G. Holden and N. W. Tschoegl, eds., "Blocks Copolymers", Interscience, New York, 1969 (J. Polymer Sci., C. 26).
7. S. L. Aggarwal, ed., "Block Polymers", Plenum, New York, 1970.
8. G. E. Molau, ed., "Colloidal and Morphological Behavior of Block and Graft Copolymers", Plenum, New York, 1971.
9. P. F. Bruins, "Polymer Blends", Interscience, New York, 1970.
10. N. A. J. Platzner, ed., "Multicomponent Systems", (Advances in Chemistry Series, No. 99), American Chemical Society, Washington, D.C. 1971.
11. D. C. Allport and W. H. Janes, eds., "Block Copolymers", Wiley, New York, 1973.
12. L. H. Sperling, ed., "Recent Advances in Polymer Blends, Grafts and Blocks", Plenum, New York, 1973.

13. J. J. Burke and V. Weiss, eds., "Block and Graft Copolymers", Syracuse Univ. Press, Syracuse, New York, 1973.
14. N. A. J. Platzner, ed., "Copolymers, Polyblends and Composites", (Advances in Chemistry Series, No. 142), American Chemical Society, Washington, D.C. 1975,
15. L. Bohn, Kolloid-Z., 213, 55 (1966); Rubber Chem. Tech., 41, 495 (1968).
16. G. M. Estes, S. L. Cooper and A. V. Tobolsky, J. Macromol. Sci., C4, 313 (1970).
17. S. L. Aggarwal, Polymer, 17, 938 (1976).
18. S. Krause, J. Macromol. Sci., C7, 251 (1972).
19. M. B. Bever and M. Shen, Materials Sci. Eng., 15, 145 (1974).
20. R. L. Scott, J. Chem. Phys., 17, 279 (1949).
21. H. Tompa, Trans. Faraday Soc., 45, 1142 (1949).
22. P. J. Flory, "Principles of Polymer Chemistry", Cornell Univ. Press, Ithaca, N.Y., 1953.
23. I. Prigogine, "The Molecular Theory of Solutions", North Holland, Amsterdam, 1957.
24. P. J. Flory, J. Am. Chem. Soc., 87, 1833 (1965).
25. P. J. Flory, B. E., Eichinger and R. A. Orwell, Macromol., 1, 287 (1958).
26. L. P. McMaster, Macromol., 6, 760 (1973).
27. S. Krause, Macromol., 3, 84 (1970).
28. N. G. Gaylord, in ref. 14, p.76
29. C. W. Childers and G. Kraus, Rubber Chem. Tech., 40 1183 (1967).

30. J. Stoelting, F. E. Karasz and W. J. MacKnight, *Polymer Sci. Eng.*, 10, 133 (1970).
31. K. Kato, J. Electron Microscopy, 14, 219 (1965); *Polymer Letters*, 4, 35 (1966).
32. H. Hendus, K. H. Illers and E. Ropte, *Kolloid Z.u.Z.f. Polym.*, 216, 110 (1967).
33. G. E. Molau and H. Keskkula, *J. Polymer Sci., Part A-1*, 4, 1595 (1966).
34. M. Matsuo, *Polymer*, 7, 421 (1966); *Polymer Eng. Sci.*, 9, 106 (1969).
35. J. F. Beecher, L. Marker, R. D. Bradford and S. L. Aggarwal, in ref. 6, p. 117.
36. T. Inoue, T. Soen, T. Hashimoto and H. Kawai, *J. Polymer Sci., part A-2*, 17, 1283 (1969).
37. H. Keskkula and P. A. Traylor, *J. Appl. Polymer Sci.*, 11, 2361 (1967).
38. E. R. Wagner, *Rubber Chem. Tech.*, 43, 1129 (1970).
39. M. Matsuo, T. K. Kwei, D. Klempner and H. L. Frisch, *Polymer Eng. Sci.*, 10, 327 (1970).
40. V. Huelck, D. A. Thomas, and L. H. Sperling, *Macromol.*, 5, 340 (1972).
41. D. McIntyre and E. Campos-Lopez, in ref. 7, p. 19.
42. H. Kim, *Macromol.*, 5, 594 (1972).
43. T. Hashimoto, K. Nagatoshi, A. Todo, H. Hasegawa and H. Kawai, *Macromol.*, 7, 364 (1974).
44. G. E. Molau, in ref. 7, p. 79.
45. M. Matsuo and S. Sagaye, in ref. 8, p. 1
46. G. E. Molau, and W. M. Wittbrodt, *Macromol.*, 1, 260 (1968).

47. E. B. Bradford, in ref. 8, p. 21.
48. L. Toy, M. Niinomi, and M. Shen, J. Macromol. Sci.-Phys., 11, 281 (1975).
49. G. A. Harpell, and C. E. Wilkes, in ref. 6, p. 31.
50. M. Niinomi, G. Akovali and M. Shen, J. Macromol. Sci.-Phys., in press.
51. E. Fischer, J. Macromol. Sci. - Chem., A2, 1285 (1968).
52. G. Kampf, M. Hoffman and H. Kromer, Ber. Bunsenges. Phys. Chem., 74, 851 (1970); J. Macromol. Sci., Phys., B6, 167 (1972).
53. J. Dlugosz, A. Keller and E. Pedemonte, Kolloid. Z.u.Z.f. Polym., 242, 1125 (1970).
54. J. Dlugosz, M.J.Folkes and A. Keller, J. Polymer Sci., -Phys., 11, 929 (1973); *ibid.*, 14, 861 (1976).
55. D. McIntyre and E. Campos-Lopez, Macromol., 3, 322 (1970).
56. E. Campos-Lopez, D. McIntyre and L. J. Fetters, Macromol. 6, 415 (1973).
57. P. R. Lewis and C. Price, Polymer, 13, 20 (1972).
58. C. Price, R. Singleton and D. Woods, Polymer, 15, 137 (1974).
59. E. Pedemonte, A. Turturro, U. Bianchi and P. Devetta, Polymer, 14, 145 (1973).
60. M. J. Folkes and A. Keller, in R. N. Haward, ed., "Physics of Glassy Polymers", Wiley, New York, 1973.
61. D. J. Meier, in ref. 6, p. 81.
62. D. F. Leary and M. C. Williams, J. Polymer Sci., B8, 335 (1970); *ibid.*, Phys. Ed., 345 (1973).
63. R. T. LaFlair, Pure Appl. Chem., 8, 195 (1971).

64. T. Soen, T. Inoue, K. Miyoshi and H. Kawai, J. Polymer Sci., Part A-2, 10, 1757 (1972).
65. D. J. Meir, in ref. 13, p. 105.
66. U. Bianchi, E. Pedemonte and A. Turturro, Polymer, 11, 268 (1970).
67. E. Helfand and Y. Tagami, J. Polymer Sci., B9, 741 (1971); J. Chem., Phys., 56, 3592 (1971), *ibid.*, 57, 1812 (1972).
68. E. Helfand, Macromol., 8, 552 (1975); J. Chem. Phys., 62, 999 (1975).
69. D. F. Leary and M. C. Williams, J. Polymer Sci. - Phys. Ed., 12, 265 (1974).
70. C. I. Chung and J. C. Gale, J. Polymer Sci.- Phys., Ed., 14, 1149 (1976).
71. A. Douy, R. Mayer, R. Rossi and B. Gallot, Mol. Cryst. Liq. Cryst., 7, 103 (1971).
72. T. Hashimoto, A. Todo, H. Itoi and H. Kawai, to be published.
73. R. G. Crystal, P. E. Erhardt and J. J. O'Malley, in ref. 7, p. 179.
74. A. K. Fritzsche and F. P. Price, in ref. 5, 249.
75. R. G. Crystal, in ref. 8, p. 279.
76. J. A. Koutsky, N. V. Hien and S. L. Cooper, J. Polymer Sci., B8, 353 (1970).
77. M. Shen, U. Mehra, M. Niinomi, J. T. Koberstein, and S. L. Cooper, J. Appl., 45, 4185 (1974).
78. W. M. Barentsen and D. Heikens, Polymer, 14, 579 (1973); *ibid.*, 15, 119 (1974).
79. E. Hirata, T. Ijitsu, T. Soen, T. Hashimoto and H. Kawai, Polymer, 16, 249 (1975).

80. G. L. Wilkes and S. L. Samuels, in ref. 13, p. 225.
81. C. Kuo and D. McIntyre, J. Polymer Sci.-Phys., 13, 1543 (1975).
82. M. Takayanagi, S. Uemura and S. Minami, J. Polymer Sci., C5, 113 (1964).
83. H. Fujino, I. Ogawa and H. Kawai, J. Appl. Polymer Sci., 8, 2147 (1964).
84. G. Kraus, K. W. Rollman and J. T. Gruver, Macromolecules, 3, 92 (1970).
85. R. A. Dickie, J. Appl. Polymer Sci., 17, 45, 65, 79 (1973).
86. D. Kaplan and N. W. Tschoegl, Polymer Eng. Sci., 14, 43 (1974).
87. E. F. Jordan, Jr., B. Artymyshyn and G. R. Riser, J. Appl. Polymer Sci., 20, 2757 (1976).
88. A. Y. Coran and R. Patel, J. Appl. Polymer Sci., 20, 3005 (1976).
89. E. H. Kerner, Proc. Phys. Soc., 69B, 808 (1956).
90. R. M. Christensen, J. Mech. Phys. Solids, 11, 127 (1963).
91. J. E. Ashton, J. C. Halpin and P. H. Petit, "Primer on Composite Analysis", Technomic Publ. Co., Stamford, Conn. 1969, Chap. 5.
92. J. C. Halpin, J. Compos. Mater., 3, 732 (1969).
93. L. E. Nielsen, J. Appl. Phys., 41, 4626 (1970).
94. L. E. Nielsen, Rheol. Acta, 13, 86 (1974).
95. S. L. Rosen, Polymer Eng. Sci., 7, 115 (1967).
96. H. Keskkula, Appl. Polymer Symp., 15, 51 (1970).
97. R. N. Haward, Br. Polymer J., 2, 209 (1970).
98. G. Holden, in ref. 11, p. 133.

99. S. L. Aggarwal, R. A. Livigni, L. F. Marker and T. J. Dudek, in ref. 13, p. 157.
100. T. L. Smith and R. A. Dickie, in ref. 6, p. 163.
101. G. Kraus and C. W. Childers, Rubber Chem. Tech., 40, 1183 (1967).
102. C. E. Bucknall, Br. Plastics, 40, 84, 118 (1967).
103. R. E. Cunningham and M. R. Treiber, J. Appl. Polymer Sci., 12, 23 (1968).
104. T. Inoue, H. Ishihara, H. Kawai, Y. Ito and K. Kato, "Mechanical Behavior of Materials", Vol. 3, Society of Materials Science - Japan, Tokyo, 1972, p. 149.
105. G. Akovali, J. Diamant and M. Shen, J. Macromol. Sci.-Phys., in press.
106. H. Kawai, to be published.
107. J. M. Charrier and R. J. Ranchoux, Polymer Eng. Sci., 11, 381 (1971).
108. M. J. Folkes and A. Keller, Polymer, 12, 222 (1971).
109. P. R. Lewis and C. Price, Polymer, 12, 258 (1971).
110. G. Akovali, K. Biliyar and M. Shen, J. Appl. Polymer Sci., 20, 2419 (1976).
111. M. Baer, J. Polymer Sci., A2, 417 (1964).
112. A. V. Tobolsky, "Properties and Structure of Polymers", Wiley, New York, 1960.
113. J. D. Ferry, "Viscoelastic Properties of Polymers", 2nd ed., Wiley, New York, 1970.
114. J. J. Aklonis, W. J. MacKnight and M. Shen, "Introduction to Polymer Viscoelasticity", Wiley-Interscience, New York, 1972.

115. M. L. Williams, R. F. Landel and J. D. Ferry, J. Am. Chem. Soc., 77, 3701 (1955).
116. M. Shen and D. R. Hansen, J. Polymer Sci., C46, 55 (1974).
117. D. R. Hansen and M. Shen, Macromol., 8, 903 (1975).
118. M. C. Williams, Am. Inst. Chem. Eng. J., 21, 1 (1975).
119. P. E. Rouse, J. Chem. Phys., 21, 1272 (1953).
120. F. Bueche, J. Chem. Phys., 22, 603 (1954).
121. B. Zimm, J. Chem. Phys., 24, 269 (1956).
122. R. E. DeWames, W. F. Hall and M. Shen, J. Chem. Phys., 46, 2782 (1967).
123. D. R. Hansen and M. Shen, Macromol., 8, 343 (1975).
124. W. H. Stockmayer and J. W. Kennedy, Macromol., 8, 351 (1975).
125. W. F. Hall and R. E. DeWames, Macromol., 8, 349 (1975).
126. F. W. Wang, Macromol., 8, 364 (1975).
127. D. Soong and M. Shen, Macromol., in press.
128. A. V. Tobolsky and K. Murakami, J. Polymer Sci., 40, 443 (1959).
129. T. Horino, Y. Ogawa, T. Soen and H. Kawai, J. Appl. Polymer Sci., 9, 2261 (1965).
130. K. C. Rusch, J. Macromol. Sci., - Phys., B2, 421 (1968).
131. T. Soen, T. Horino, Y. Ogawa, K. Kymma and H. Kawai, J. Appl. Polymer Sci., 10, 1499 (1966).
132. M. Shen and D. H. Kaelble, J. Polymer Sci., B8, 149 (1970).
133. M. Shen, E. H. Cirilin and D. H. Kaelble, in ref. 8.

134. J. Bares and M. Pegoraro, J. Polymer Sci., Part A2, 9, 1287 (1971).
135. D. G. Fesko and N. W. Tschoegl, J. Polymer Sci., C35, 51 (1971).
136. G. Kraus, F. E. Naylor and K. W. Rollman, J. Polymer Sci., Part A-2, 9, 1839 (1971).
137. K. Lim, R. E. Cohen and N. W. Tschoegl, ref. 10, p. 397.
138. R. T. Jamieson, V. A. Kaniskin, A. C. Ouano and M. Shen, in "Advances in Polymer Science and Engineering", K. D. Pae, D. R. Morrow and Y. Chen, eds., Plenum Press, New York, 1972 p. 163.
139. C. S. Fielding-Russell, Rubber Chem. Tech., 45, 252 (1952).
140. G. Kraus, K. W. Rollman and J. O. Gardner, J. Polymer Sci.- Phys. Ed., 10, 2061 (1972).
141. V. A. Kaniskin, A. Kaya, A. Ling and M. Shen, J. Appl. Polymer Sci., 17, 2695 (1973).
142. T. Soen, T. Ono, K. Yamashita and H. Kawai, Kolloid Z.u.Z.f. Polymer, 250, 459 (1972).
143. M. Shen, V. A. Kaniskin, K. Biliyar and R. H. Boyd, J. Polymer Sci., Phys. Ed., 11, 2261 (1973).
144. A. Kaya, G. Choi and M. Shen, in "Deformation and Fracture of High Polymers", H. H. Kausch, J. A. Hassell and R. I. Jaffe, eds., Plenum Press, New York, 1974, p. 273.
145. D. G. Fesko and N. W. Tschoegl, Int. J. Polym. Mater., 3, 51 (1974).

146. T. Soen, M. Shimomura, T. Uchida and H. Kawai, Colloid Polym. Sci., 252, 933 (1974).
147. D. Kaplan and N. W. Tschoegl, Polymer Eng. Sci., 14, 43 (1974).
148. R. E. Cohen and N. W. Tschoegl, Trans. Soc., Rheol. 20, 153 (1976).
149. G. Kraus and K. W. Rollman, J. Polymer Sci.-Phys. Ed., 14 1133 (1976).
150. R. E. Cohen and N. W. Tschoegl, Int. J. Polymer Mat., 2, 49 (1972); *ibid.*, 2, 205 (1973); *ibid.*, 3, 3 (1974).
151. G. Choi, A. Kaya and M. Shen, Polymer Eng. Sci., 13, 231 (1973).
152. U. Mehra, L. Toy, K. Biliyar and M. Shen, in ref. 14, p. 399.
153. G. Kraus and K. W. Rollman, to be published.

THE AUTHORS

Mitchel Shen received his B.S. from Saint Francis College, and M.A. and Ph.D. from Princeton University. Prior to joining the Berkeley faculty in 1969, he was at the Rockwell Science Center in Thousand Oaks, California. His research interests are in the physical properties of polymers, plasma polymerization and natural macromolecules. In 1975 Mitch was a Visiting Professor of Polymer Chemistry at Kyoto University, where the preparation of this review was initiated.

Hiromichi Kawai received his undergraduate education at the Kyoto Institute of Technology. Since 1946 he has been associated with Kyoto University where he also received his doctorate degree. At present Hiro is a Professor in the Department of Polymer Chemistry there. During 1958-1960 he worked with R. S. Stein at the University of Massachusetts as a post-doctoral fellow, and since then has made numerous visits to the United States. His research interests are in the rheo-optical properties of semi-crystalline and heterophase polymers.

FIGURE CAPTIONS

Figure 1: Effects of varying molecular weights (indicated by the numerals) of the components on the phase diagram of the binary polymer mixture. Solid lines indicate binodal curves, and dashed lines spinodal curves.²⁷

Figure 2: Loss tangent as a function of temperature for block (solid line) and random (dashed line) copolymers of butadiene (75%) and styrene (25%).³¹

Figure 3: Schematic diagram demonstrating the five types of fundamental domain structures in polymeric alloys as a function of changing fractional compositions of the two components.⁴⁴

Figure 4: Electron micrographs ³⁶ of diblock copolymers of styrene and isoprene cast from toluene and cut normal to the surfaces: (a) 20% styrene; (b) 40% styrene; (c) 50% styrene; (d) 60% styrene; (e) 60% styrene, but cut in a direction normal to case d; (f) 70% styrene.

Figure 5: Electron micrographs ³⁶ of the diblock copolymer of styrene and isoprene containing 40% styrene and cast from (a) toluene; (b) methyl ethyl ketone; (c) cyclohexane; (d) carbon tetrachloride; (e) n-hexane; and (f) n-heptane.

Figure 6: Electron micrographs of the triblock copolymer of styrene and butadiene (SBS) containing 28% styrene and cast from a mixed solvent of tetrahydrofuran and methyl ethyl ketone (a) pure SBS; (b) SBS blended with low

molecular weight polystyrene; (c) SBS blended with high molecular weight polystyrene;⁵⁰ and (d) SBS blended with high molecular weight polybutadiene.⁴⁸

Figure 7: Electron micrograph⁵² of "macrolattice" of diblock copolymer of styrene and butadiene (68% styrene) and cast from xylene.

Figure 8: Schematic diagram demonstrating three types of fundamental domain structures and molecular arrangements within the domains for diblock copolymers.⁶⁴

Figure 9: Schematic diagrams demonstrating three types of fundamental domain structures and molecular arrangements within the domains for graft copolymers.⁶⁴

Figure 10: Schematic diagram of Leary-Williams model of domain formation for triblock copolymers (for rods or spheres).⁶²

Figure 11: Changes of relative minimum free energies of three types of domains (spheres, cylinders or rods, and lamellar) with fractional composition of block copolymer compositions.⁶⁴

Figure 12: Cross-polarized photomicrographs⁷⁹ of a series of triblock copolymers of ethylene oxide (EO) and isoprene cast from benzene: (a) pure PEO; (b) block copolymer containing 74.6% EO; (c) block copolymer containing 67.4% EO; and (d) block copolymer containing 52.4% EO.

Figure 13: Electron micrographs⁷⁹ of triblock copolymers of ethylene oxide and isoprene cast from benzene and stained with osmium tetroxide: (a) 74.6% EO; (b) 74.6% EO but shadowed by Pt-Pd; (c) 67.4% EO; (d) 52.4% EO; (e) 14.0% EO; and (f) 8.8% EO.

Figure 14: Schematic diagram demonstrating the domain formation and molecular arrangements within the domains for a semicrystalline block copolymer.⁷⁹

Figure 15: Replica electron micrograph ⁷⁷ of segmented polyester of tetramethylene ether glycol terephthalate (PTMEGT) and tetramethylene terephthalate sequences (4GT). (a) 54% 4GT; (b) 4GT; and (c) 81% 4GT.

Figure 16: (a) The schematic diagrams of the two-phase mixture on the left hand side are represented by the equivalent model on the right hand side; (b) Mechanical models used for calculating the modulus of the equivalent models in (a). ^{82,83}

Figure 17: Young's moduli of a series of triblock copolymers of butadiene-styrene-butadiene as a function of their volume fraction of styrene content. The curve was calculated ⁹⁴ using eq. 12.

Figure 18: Stress-strain curves for triblock copolymers of styrene-butadiene-styrene of various styrene contents.⁹⁸

Figure 19: Stress-strain curve for the diblock copolymer of styrene-isoprene (50/50) cast from a mixed solvent of toluene and methyl ethyl ketone.¹⁰⁴

Figure 20: Electron micrographs for the stretched film of the diblock copolymer of styrene-isoprene (50/50) cast from the mixed solvent of toluene and methyl ethyl ketone.

Samples were cut normal to the surface but parallel to the stretching direction at various points of the sample as indicated.¹⁰⁴

Figure 21: Stress-strain curves of the triblock copolymer of styrene-butadiene-styrene and those blended with various amounts of homopolystyrene and cast from the mixed solvent of tetrahydrofuran/methyl ethyl ketone.¹⁰⁵

Figure 22: Electron micrograph of triblock copolymer of styrene-butadiene-styrene cast from tetrahydrofuran/methyl ethyl ketone, stretched to 500% and stained with OsO_4 . The strain was recovered to 200% at the time when the photograph was taken.¹⁰⁶

Figure 23: Cyclic stress-strain curves of the triblock copolymer of styrene-butadiene-styrene cast from tetrahydrofuran/methyl ethyl ketone.¹⁰⁶

Figure 24: Stress-strain behavior of a molded and sheared triblock copolymer of styrene-butadiene-styrene in the longitudinal and transverse directions of flow.¹⁰⁷

Figure 25: Stress-strain curves of a macrolattice of triblock copolymer of styrene-butadiene-styrene in longitudinal and transverse directions of the cylindrical domains.¹⁰⁸

Figure 26: Stress-strain curves of poly(methyl methacrylate) and gradient polymers prepared from diffusion polymerization of methyl acrylate in poly(methyl methacrylate).¹¹⁰

Figure 27: Stress-strain curves at various temperatures of interpenetrating networks of 20% methyl acrylate in poly(methyl methacrylate) and gradient polymers of comparable composition.¹¹⁰

Figure 28: Dynamic storage moduli and loss tangent of a 1-1 polyblend of polystyrene and poly(α -methyl styrene) and a diblock copolymer of the same composition.¹¹¹

Figure 29: Stress-relaxation isotherms and viscoelastic master curve of a triblock copolymer of styrene- α -methylstyrene-styrene containing 5% α -methylstyrene.¹¹⁶

Figure 30: Time-temperature shift factors for a series of triblock copolymers of styrene- α -methylstyrene-styrene, containing 5% up to 65% α -methylstyrene (Samples A to E) and for a triblock copolymer of α -methylstyrene-styrene- α -methylstyrene containing 27% α -methylstyrene (Sample F).¹¹⁷

Figure 31: Maximum relaxation times, reduced by that of pure polystyrene, for block copolymers as a function of composition. Open circles triblock copolymer of styrene- α -methylstyrene-styrene; Closed circle diblock copolymer of styrene- α -methylstyrene; Triangle: triblock copolymer of α -methylstyrene-styrene- α -methylstyrene.^{117,127}
Curves were computed from theory.¹²³

Figure 32: Stress-relaxation isotherms of a triblock copolymer of styrene-butadiene-styrene (Kraton 1101) cast from a mixed solvent of tetrahydrofuran and methyl ethyl ketone.¹¹¹

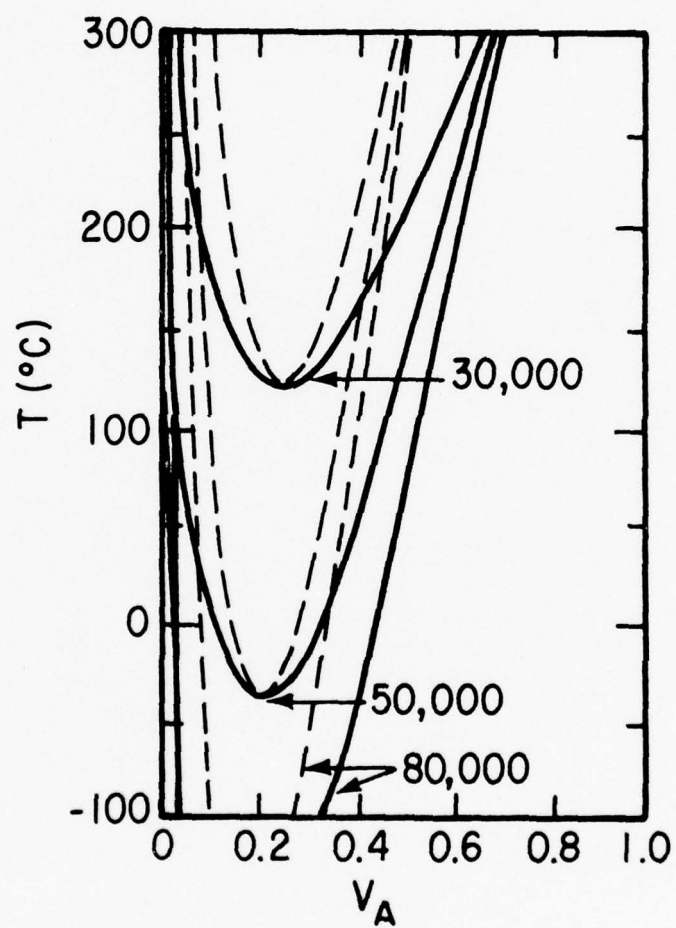
Figure 33: Viscoelastic master curve obtained by simple horizontal shifting of the stress-relaxation isotherms in Figure 32. Filled circles are data separately determined by stress-relaxation to long times. The open circle is the value measured by acoustic spectrometer at kilocycle frequency.¹¹¹

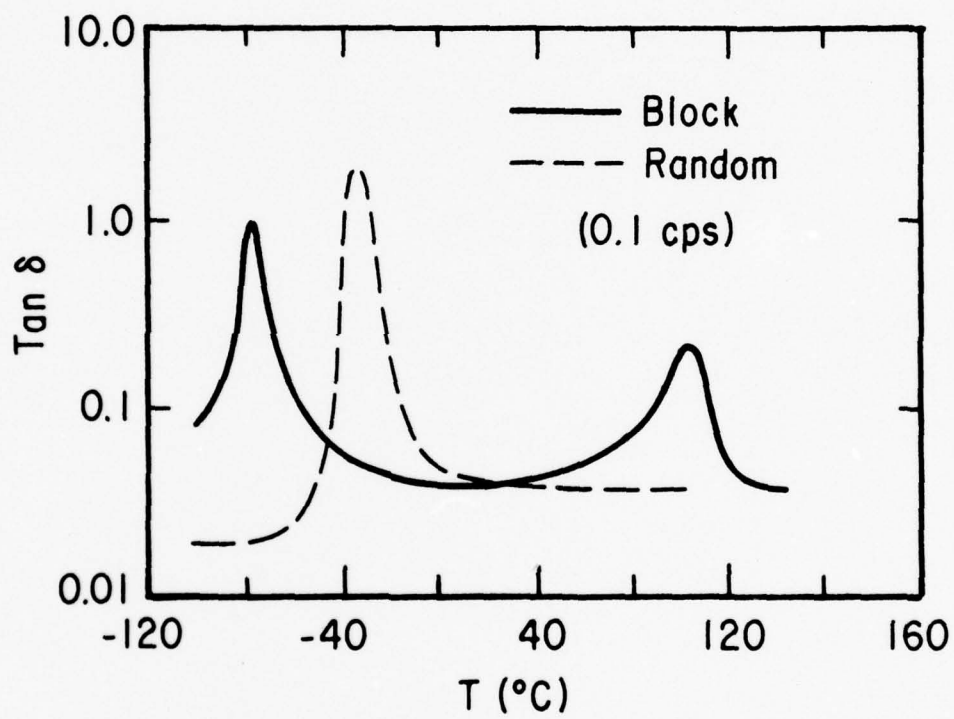
Figure 34: Time-temperature shift factor data for the triblock copolymer of styrene-butadiene-styrene (Kraton 1101) cast from a mixed solvent of tetrahydrofuran and methyl ethyl ketone.¹¹¹

Figure 35: Schematic diagram of the weighting factors for the time-temperature shift factors of a heterogeneous material.¹³⁵

Figure 36: Loss tangent as a function of temperature for a triblock copolymer of styrene-butadiene-styrene (Kraton 1101) cast from a mixed solvent of tetrahydrofuran and methyl ethyl ketone. Filled circles are calculated from the master curve in Figure 33, and the broken line is the ultrasonic data.¹⁴³

Figure 37: Loss moduli as a function of frequency for a branched block copolymers $(SB)_n$, and its blends with polybutadienes. Numerals designate the molecular weights of the homopolymers (in thousands). All polyblends contain 33.3% of PB, and solution cast from toluene. High frequency data were determined by dynamic mechanical measurements, and low frequency by stress-relaxation.¹⁵³ Broken line indicate extrapolated data.



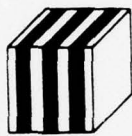




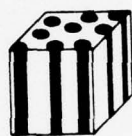
A
SPHERES



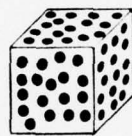
A
CYLINDERS



A, B
LAMELLAE



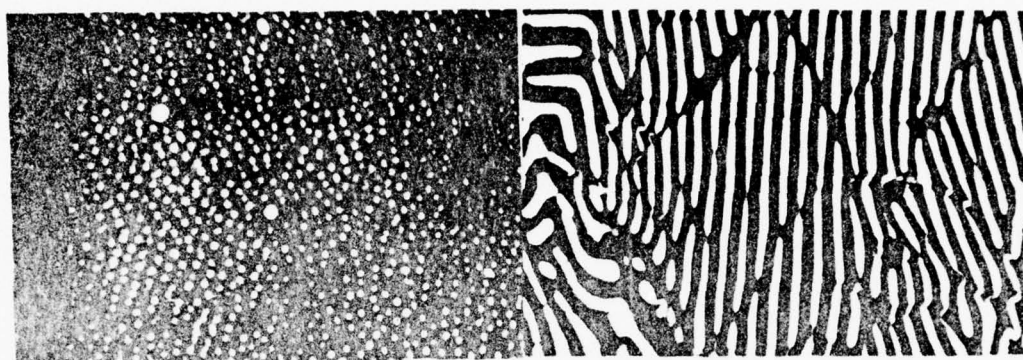
B
CYLINDERS



B
SPHERES

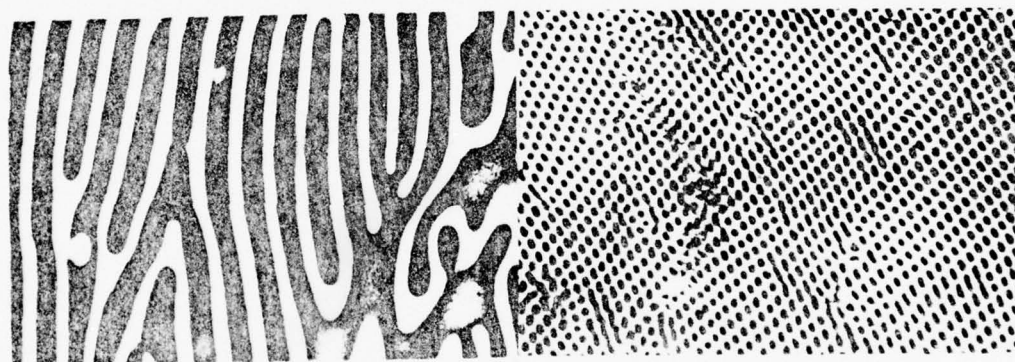
Increasing A - Content
Decreasing B - Content →

— 1 μ —



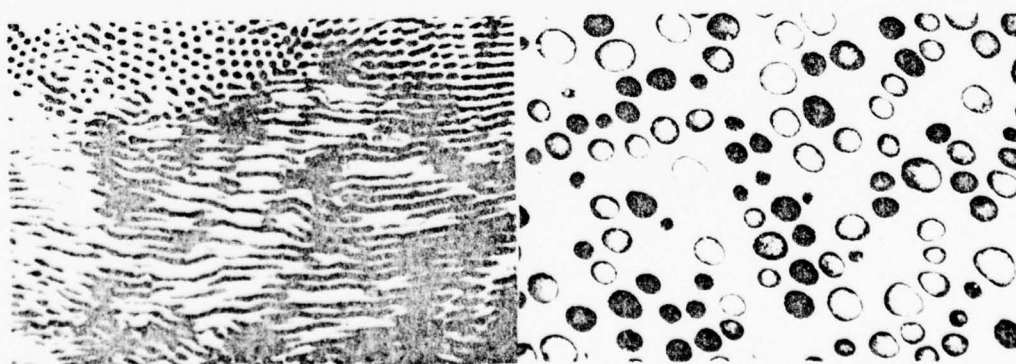
(a) (SI-1, 20/80 Sty-Isop)

(b) (SI-2, 40/60 Sty-Isop)



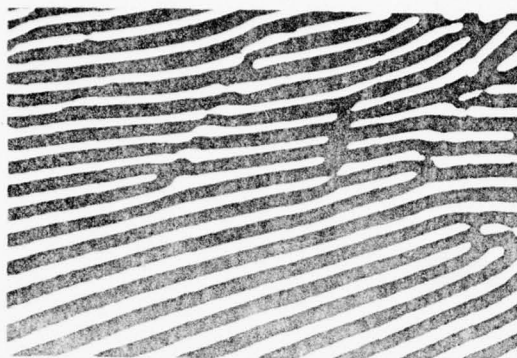
(c) (SI-3, 50/50 Sty-Isop)

(d) (SI-4, 60/40 Sty-Isop)



(e) (SI-4, 60/40 Sty-Isop)

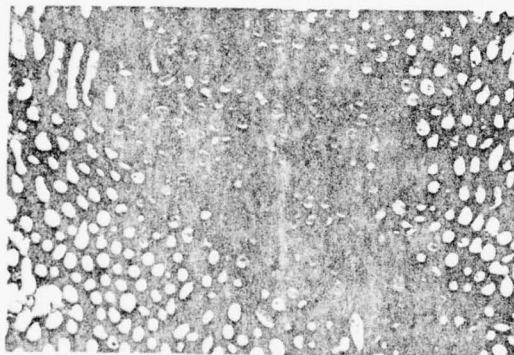
(f) (SI-5, 70/30 Sty-Isop)



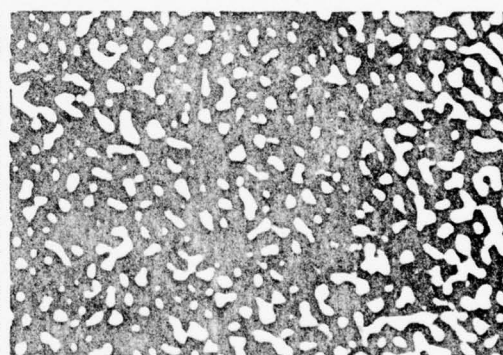
(a) (SI-2, Toluene)



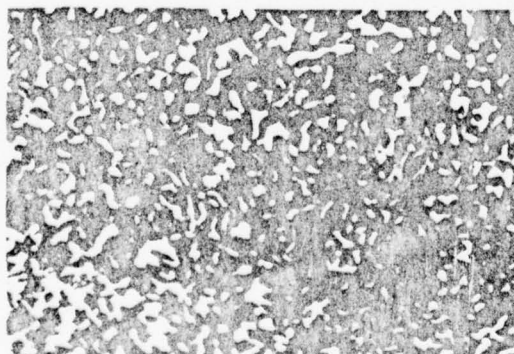
(b) (SI-2, MEK)



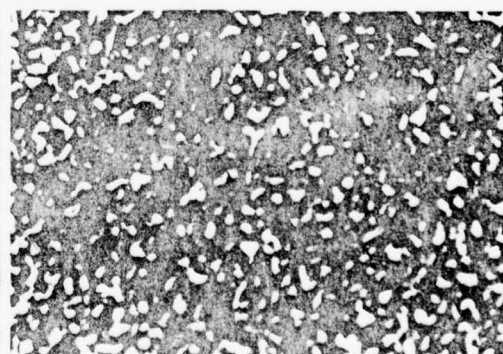
(c) (SI-2, Cyclohexane)



(d) (SI-2, CCl_4)

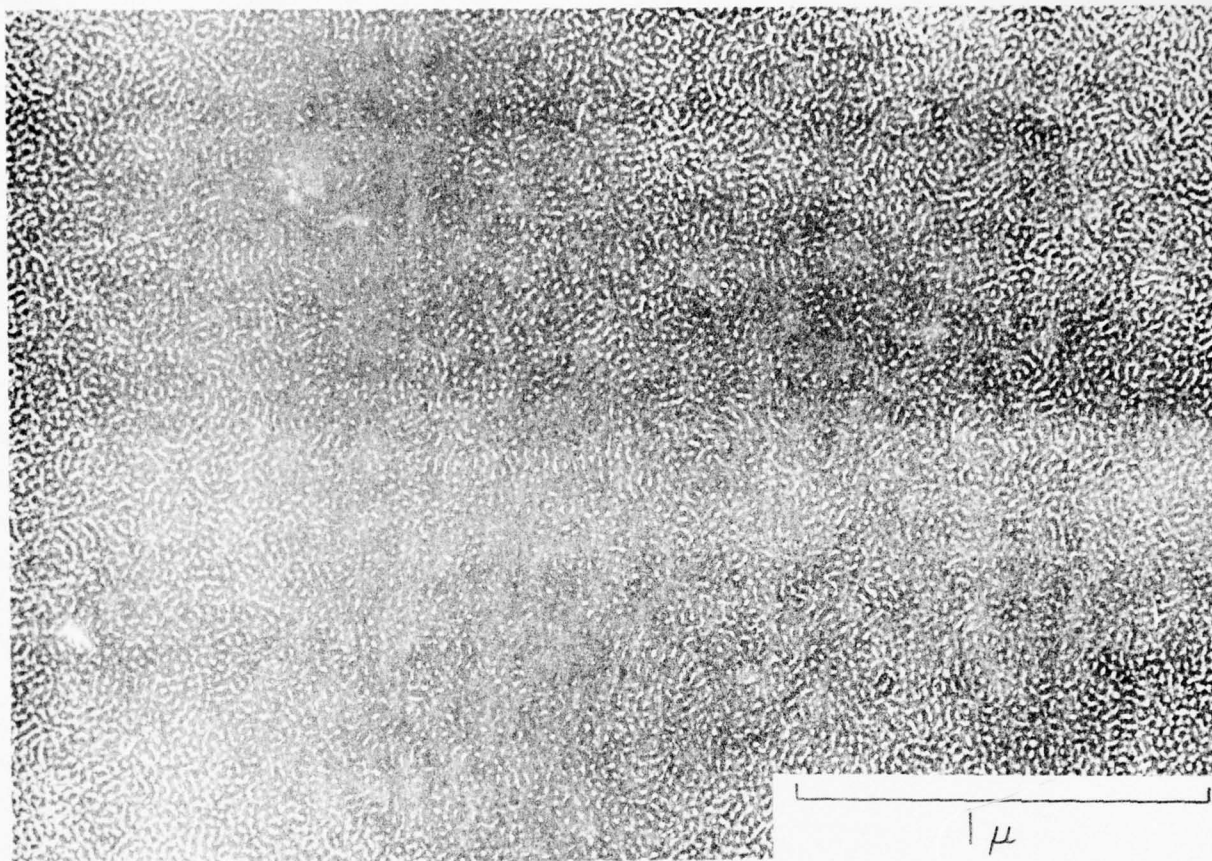


(e) (SI-2, n-hexane)

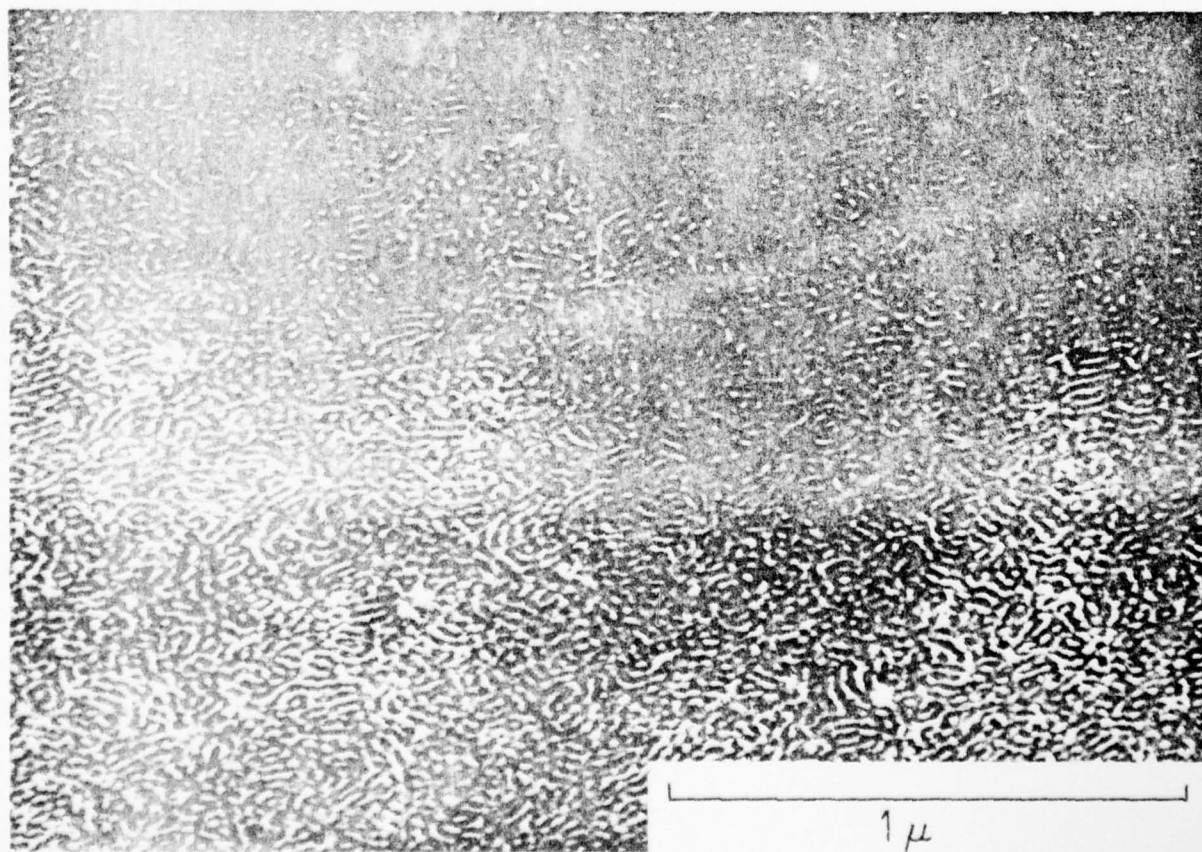


(f) (SI-2, n-heptane)

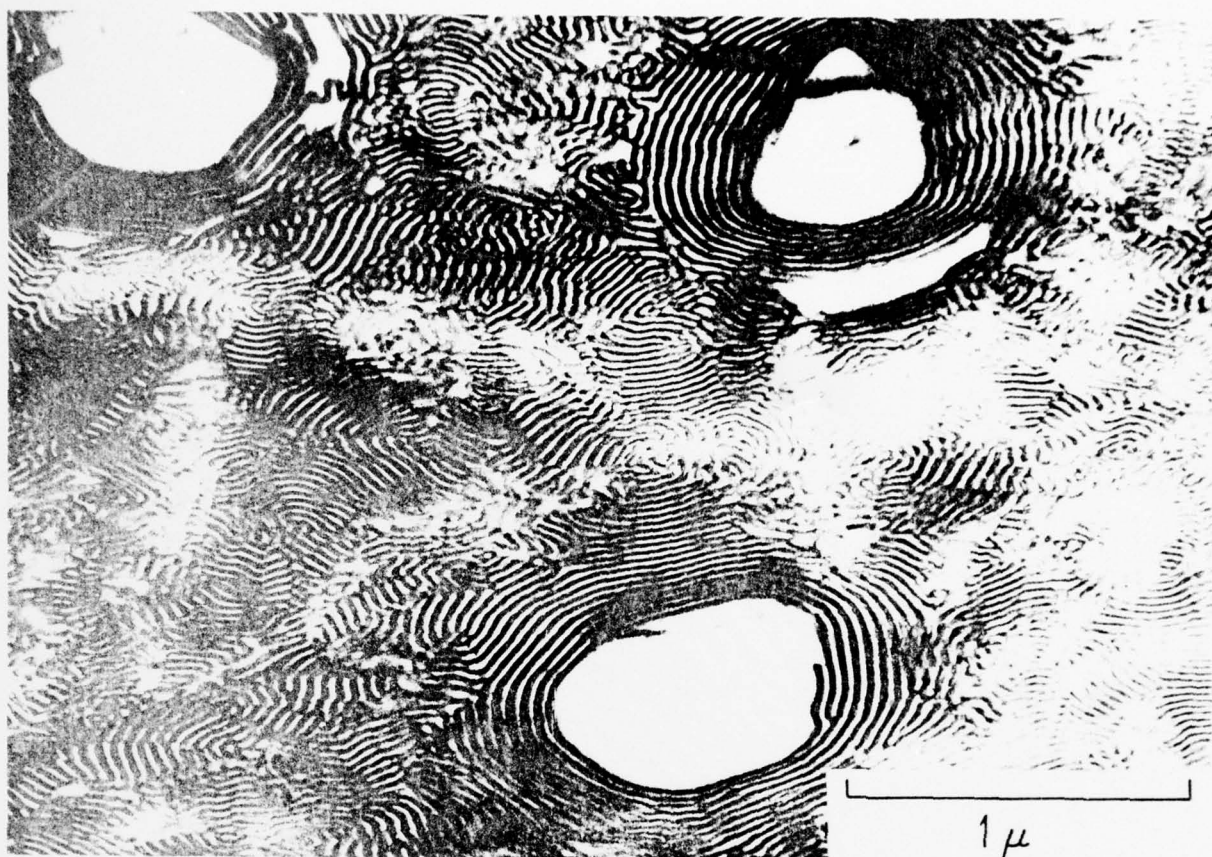
(A)



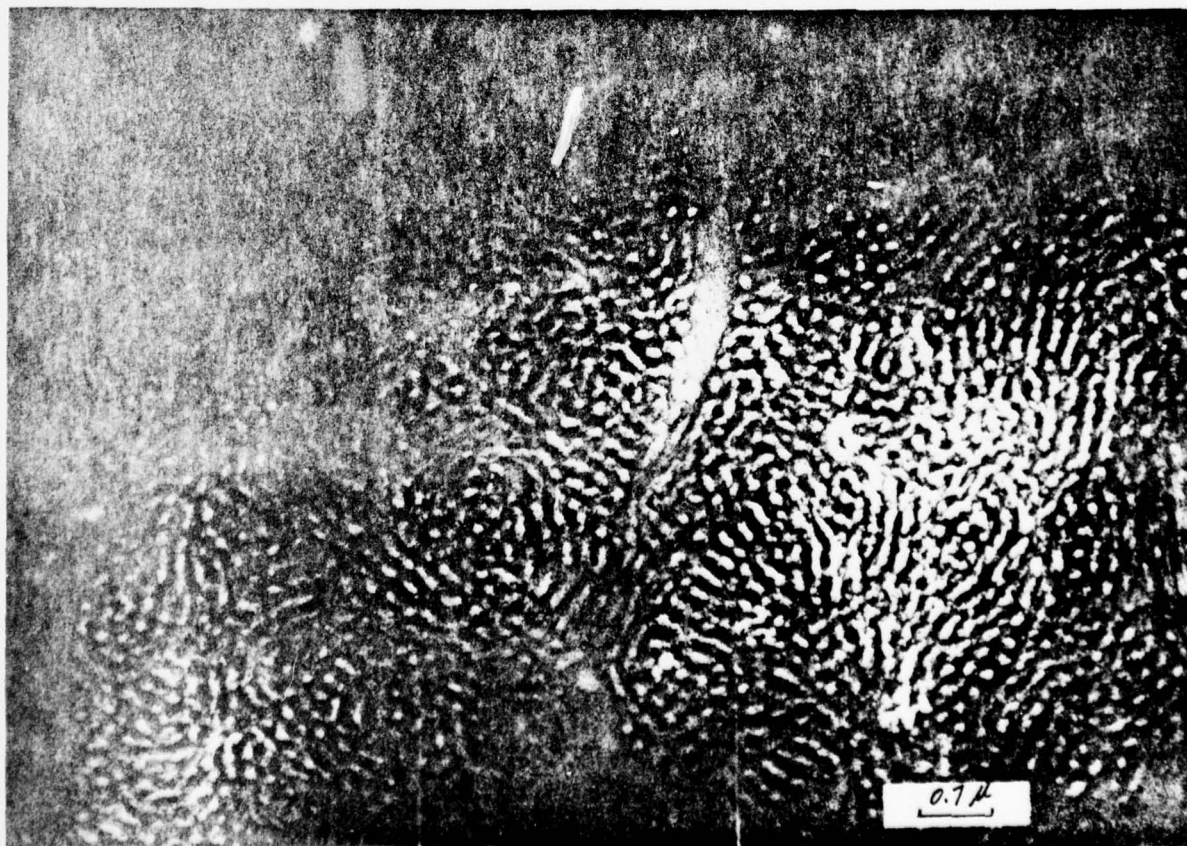
(B)

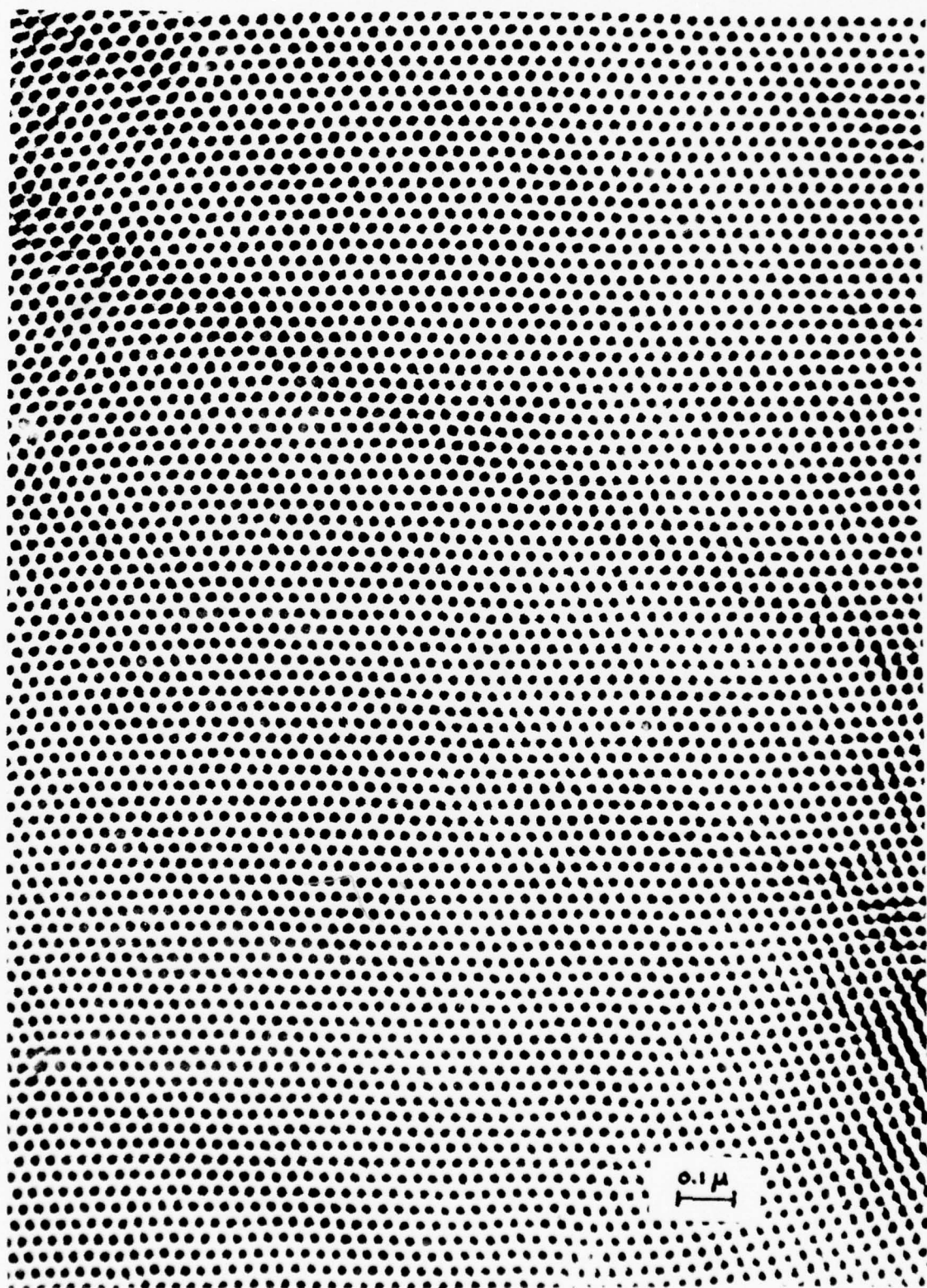


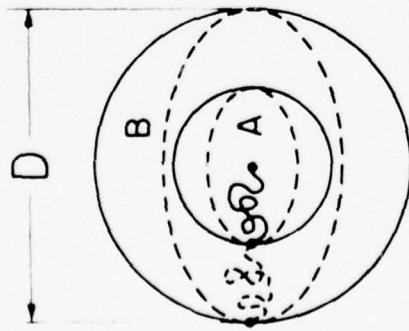
(C)



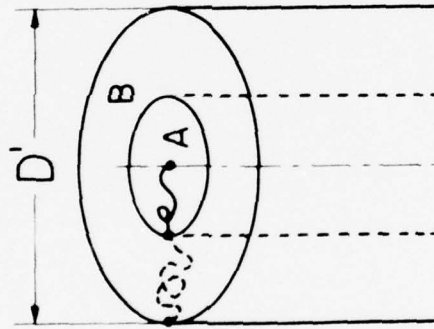
(D)



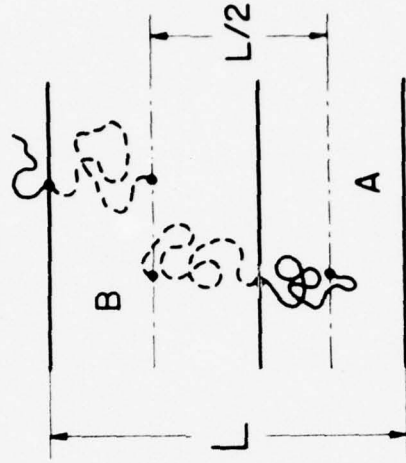




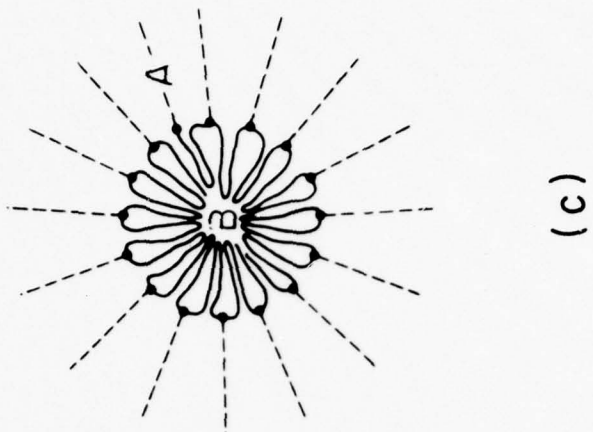
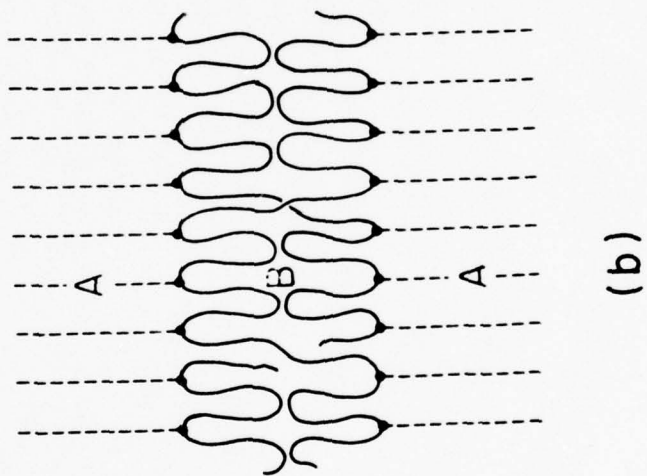
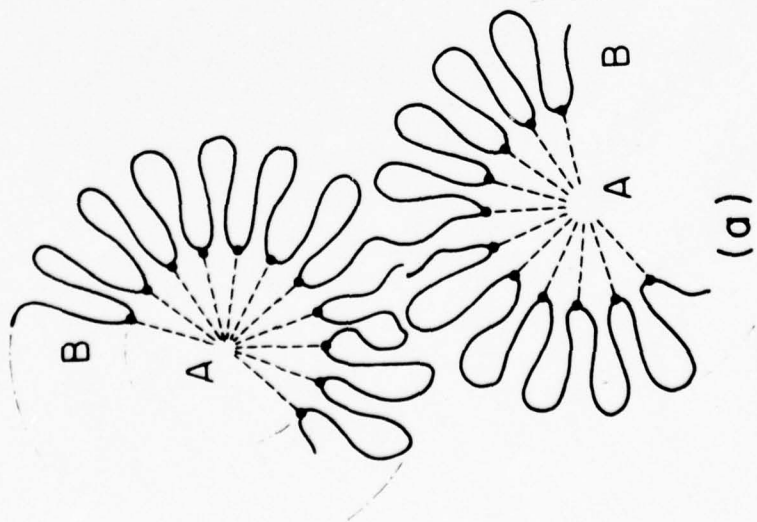
(a) spherical micelle

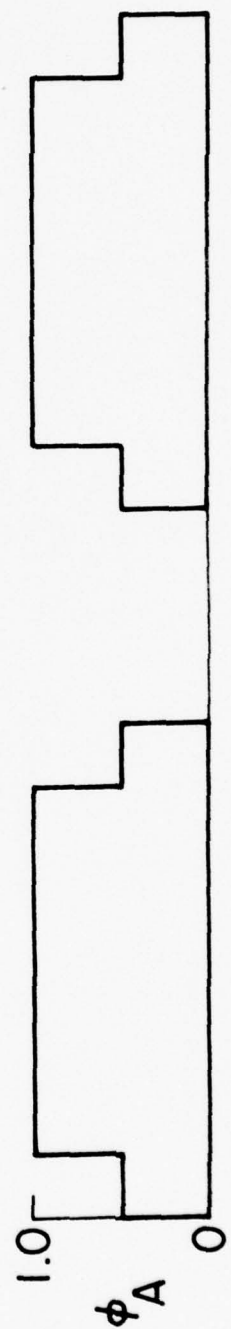
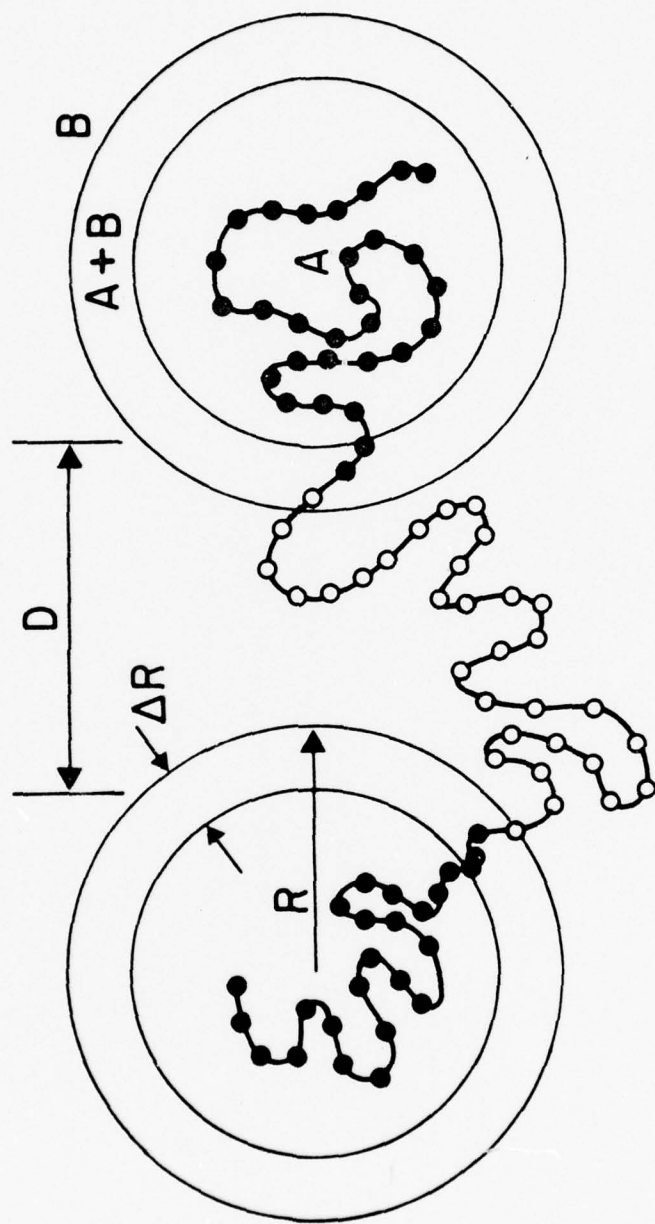


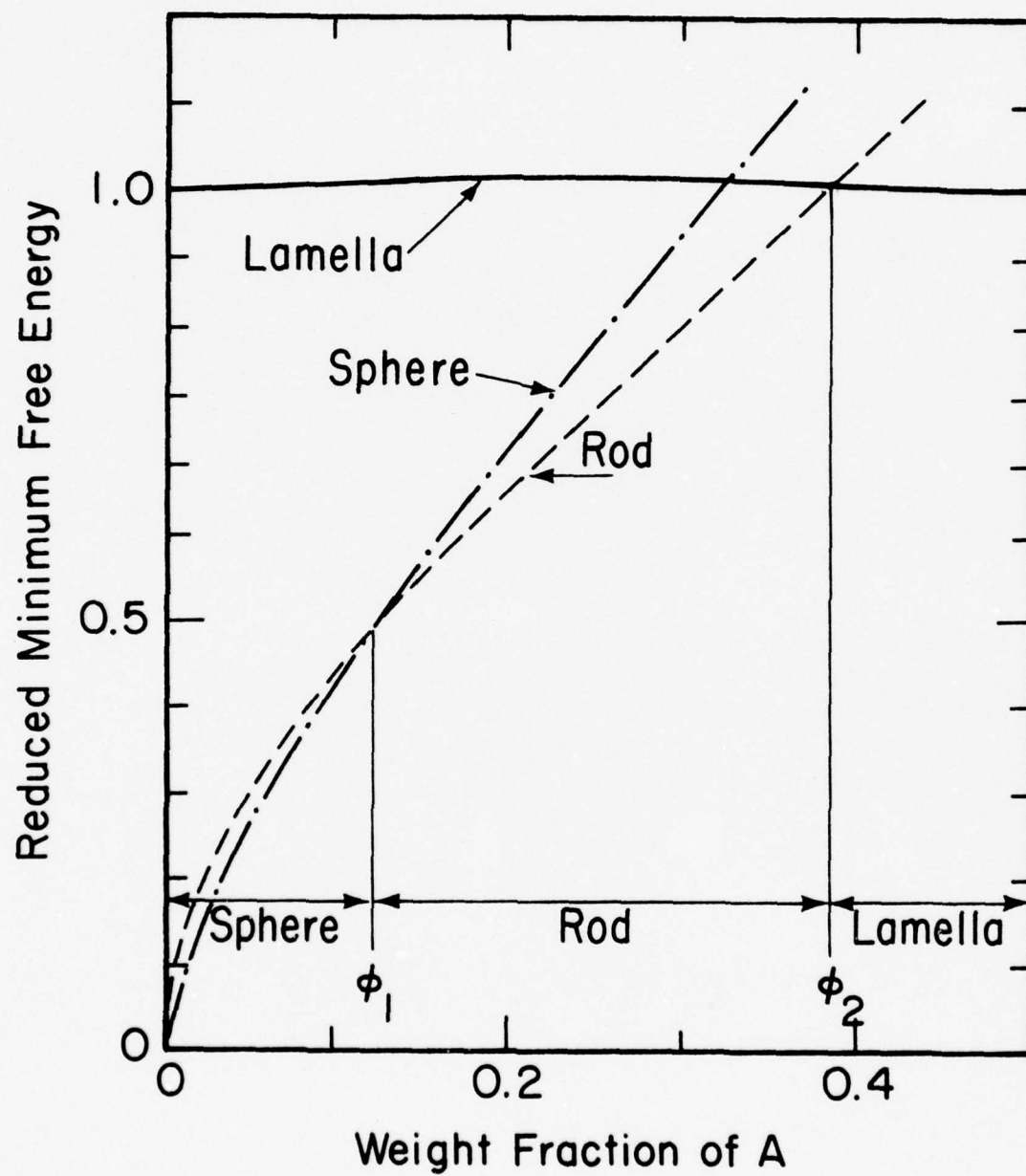
(b) rod-like micelle



(c) lamellar micelle



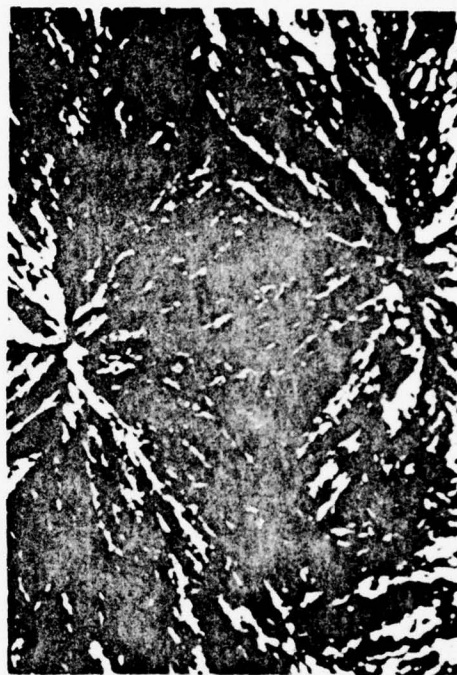




—50μ—



(b) E0/Ip/E0-2



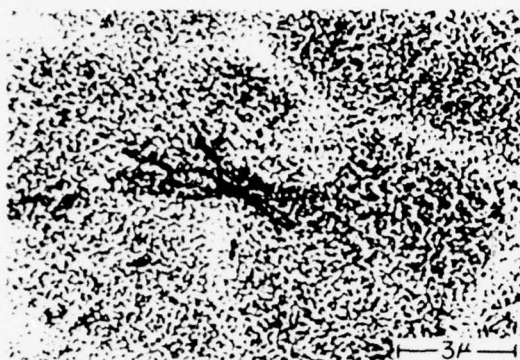
(d) E0/Ip/E0-4



(a) Homo-PE0



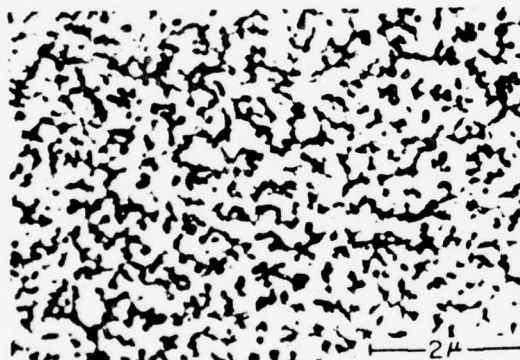
(c) E0/Ip/E0-3



(a) E0/Ip/E0-2



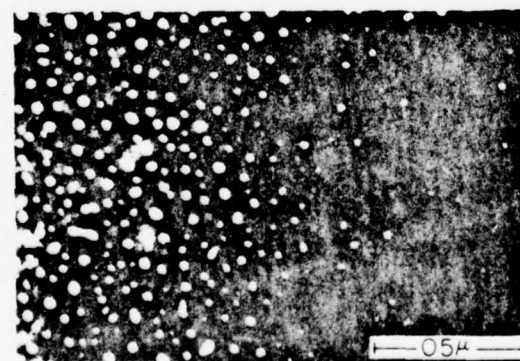
(b) E0/Ip/E0-2



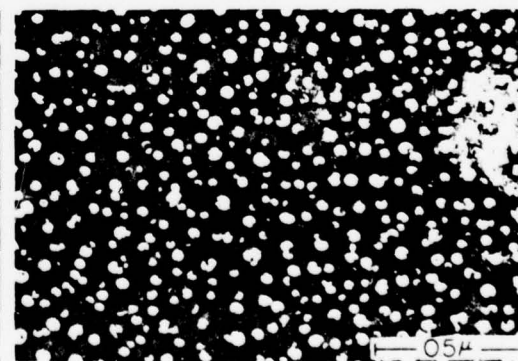
(c) E0/Ip/E0-3



(d) E0/Ip/E0-4



(e) E0/Ip/E0-5



(f) E0/Ip/E0-7

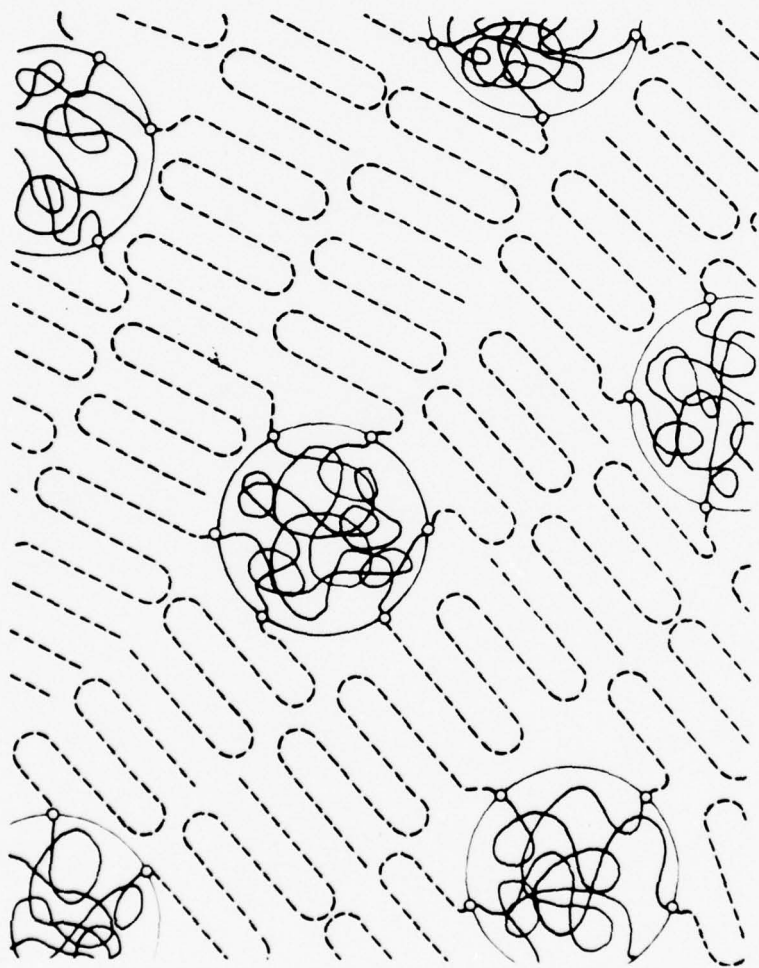
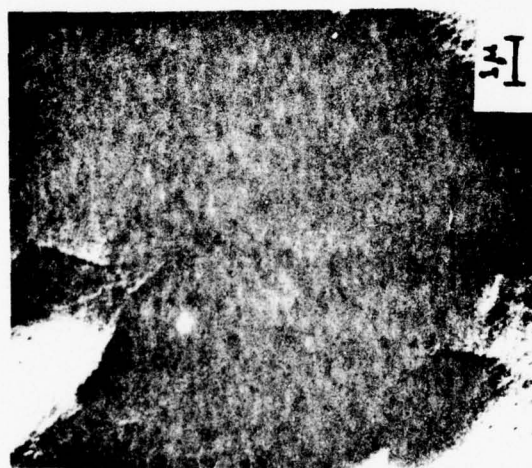


Fig. 15



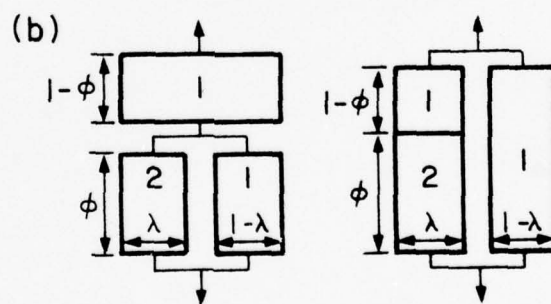
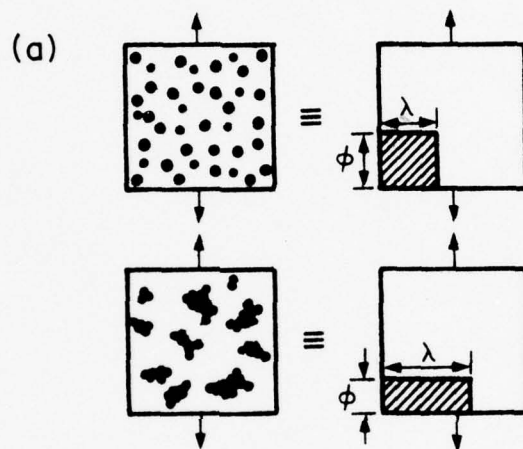
(C)



(B)



(A)



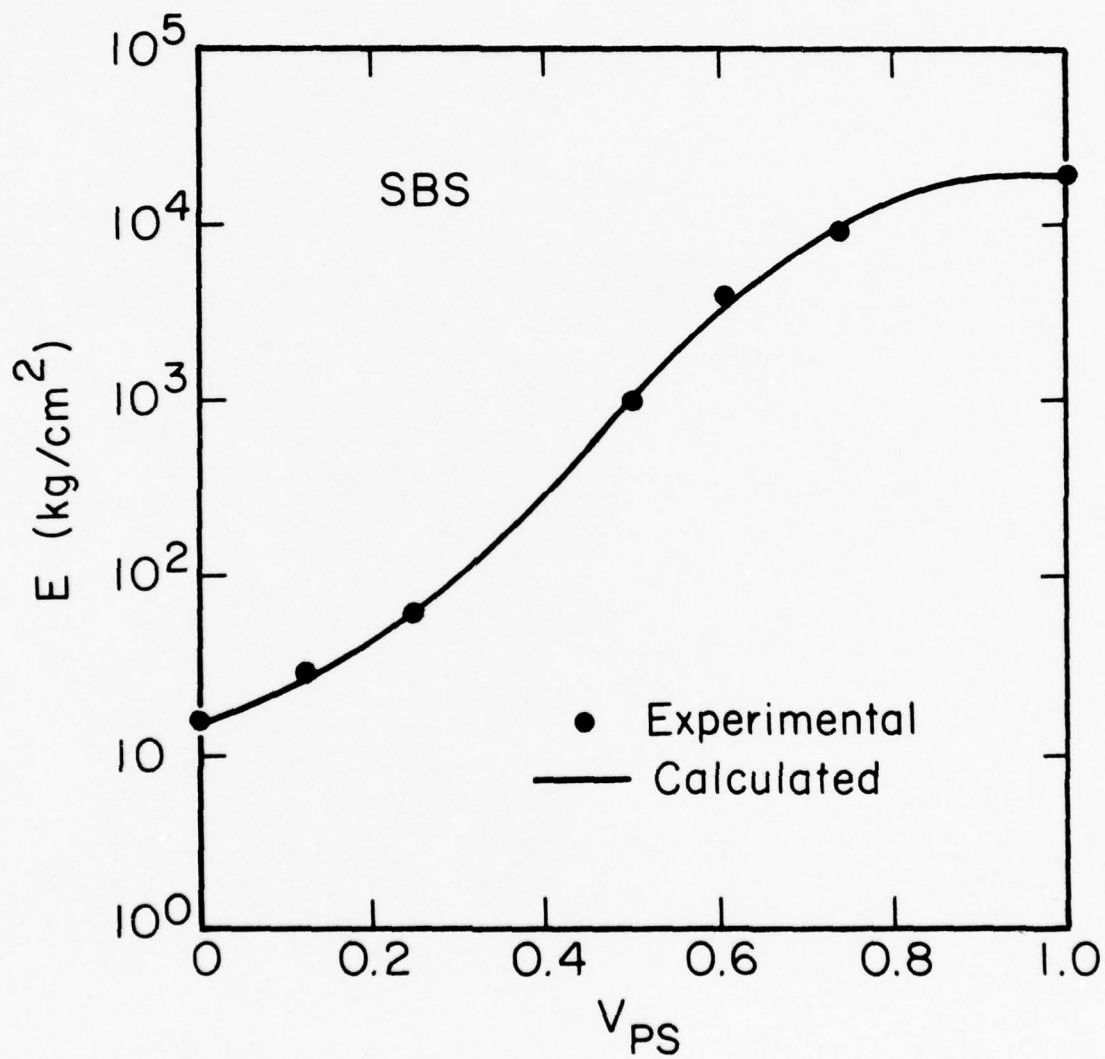
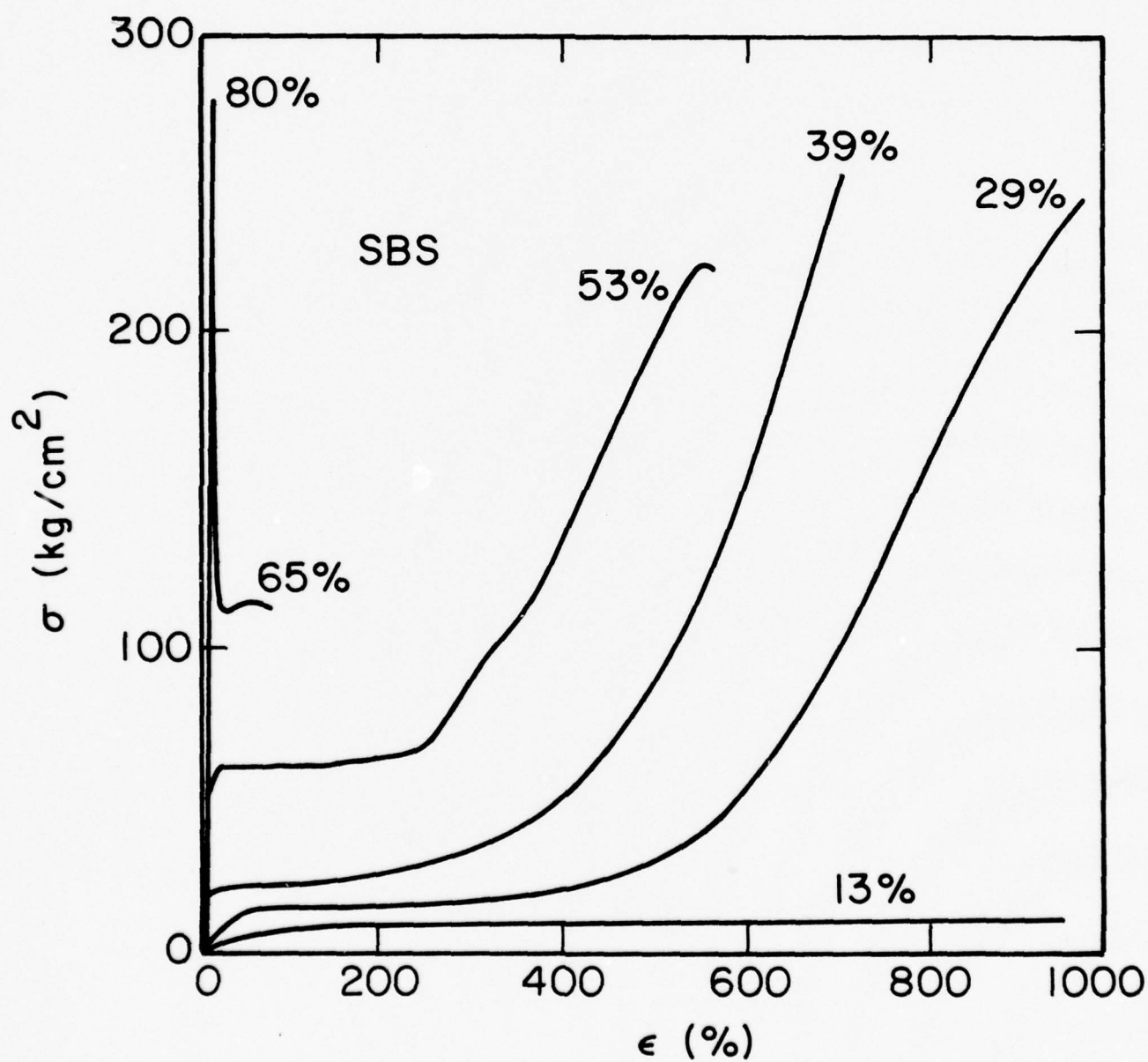
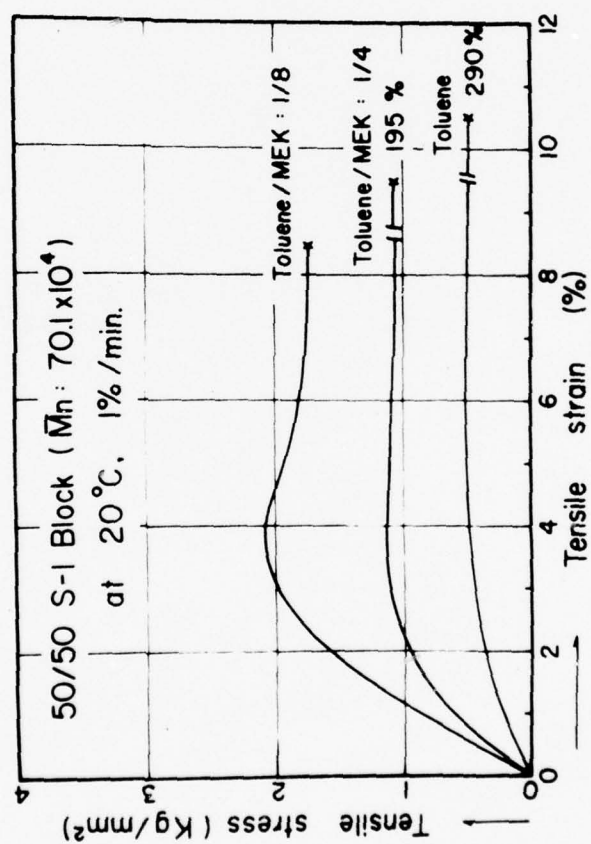
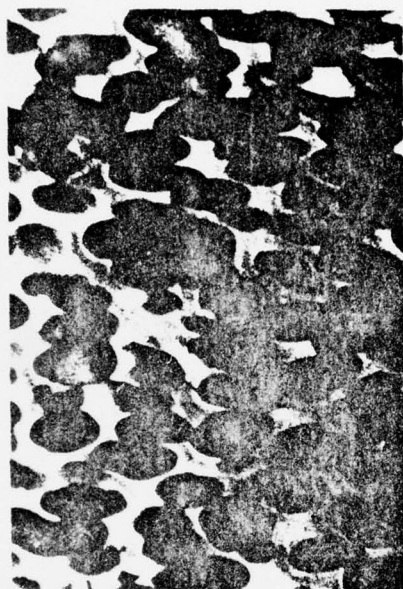
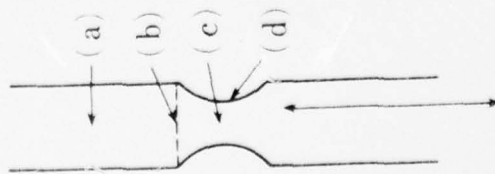


Fig. 18







(b)



(a)

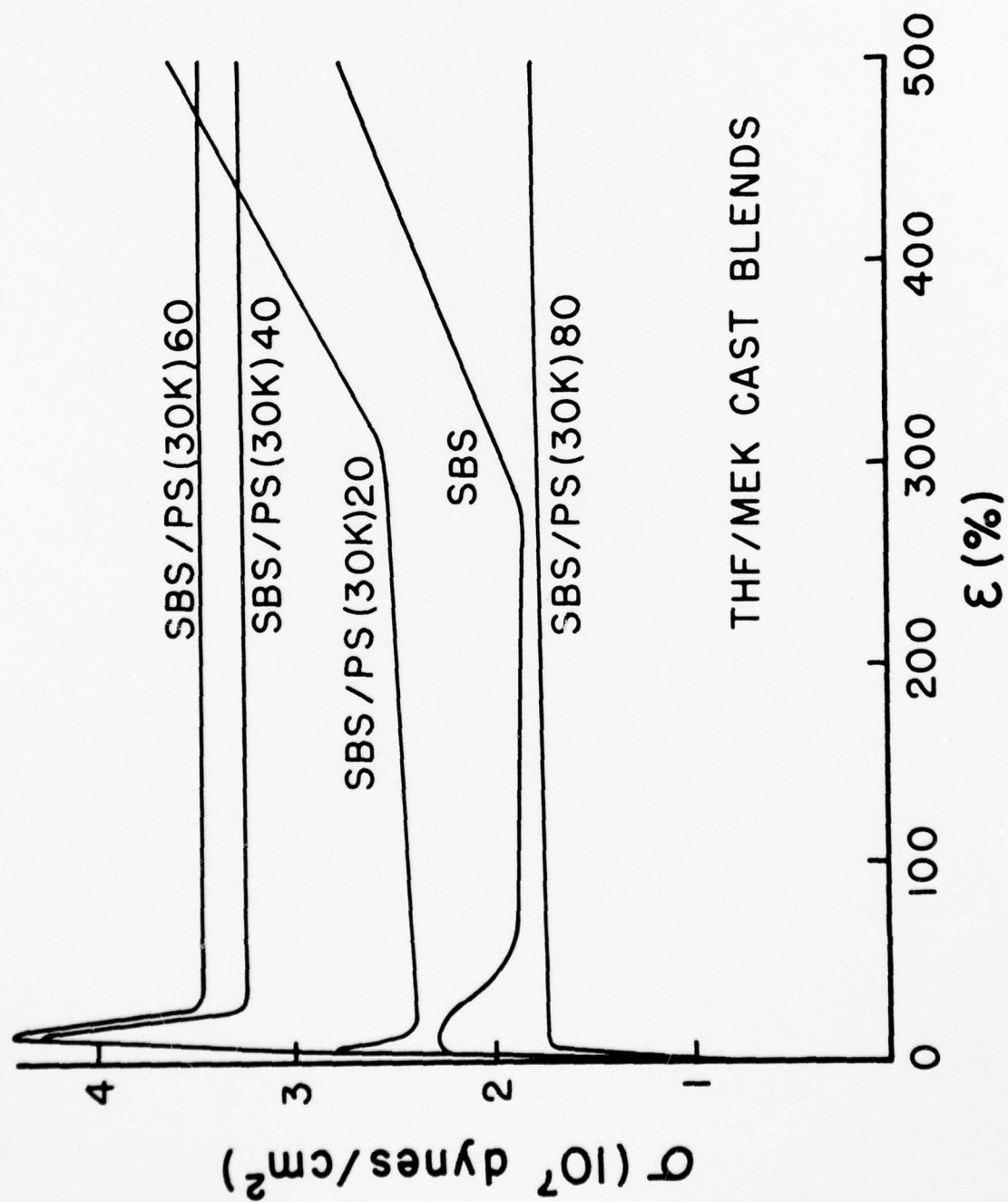


(d)

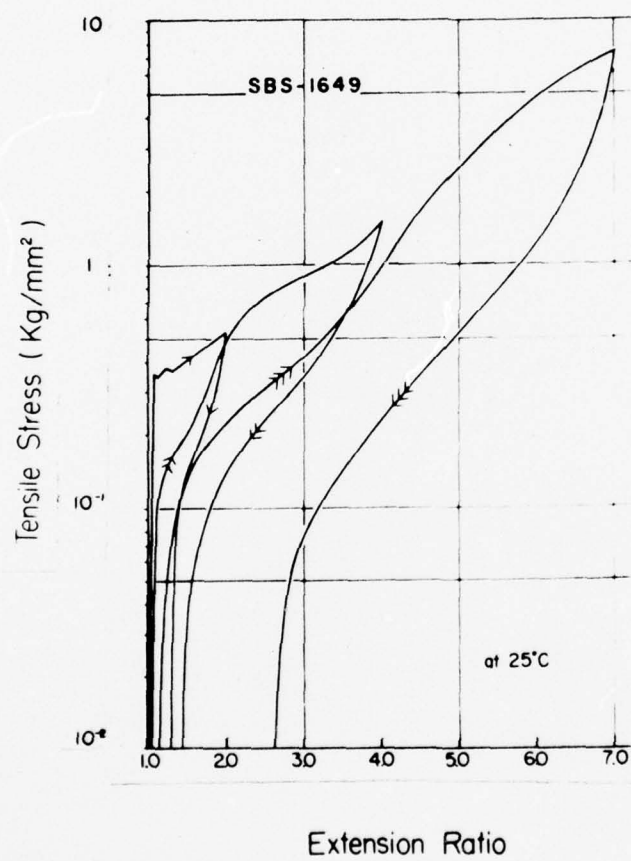


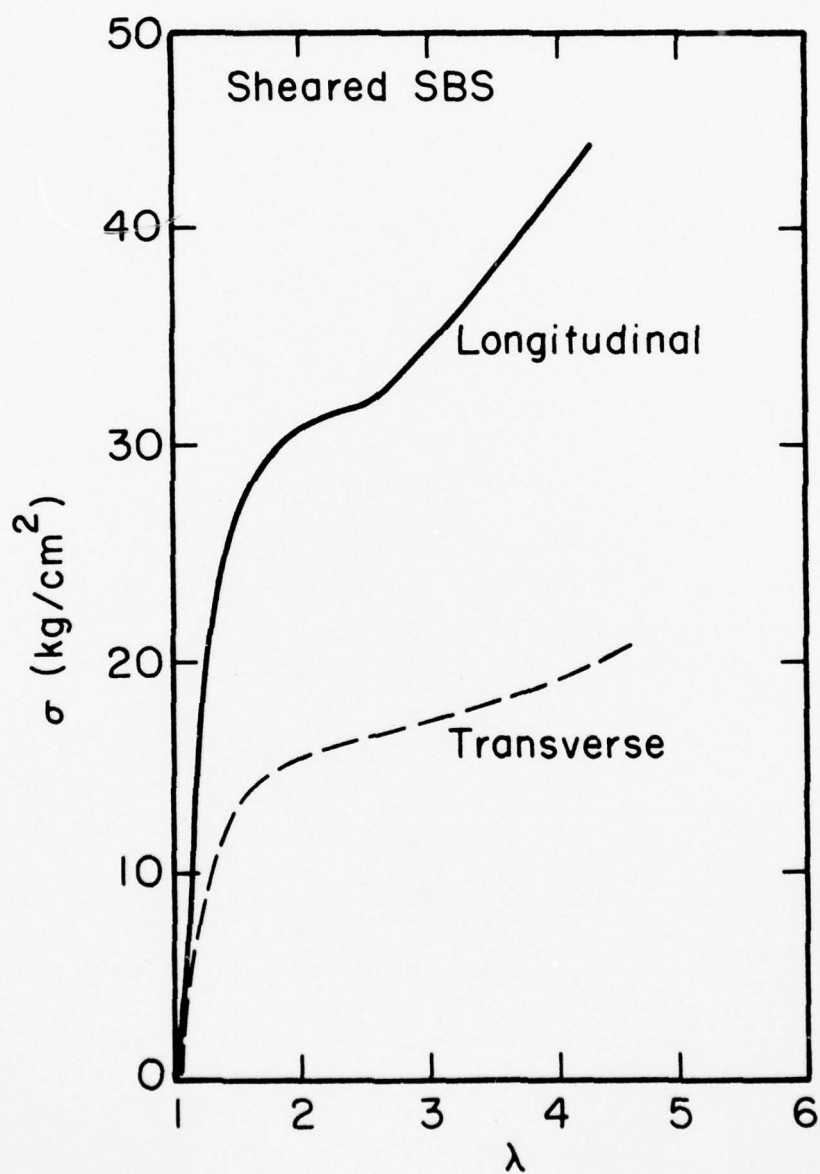
(c)

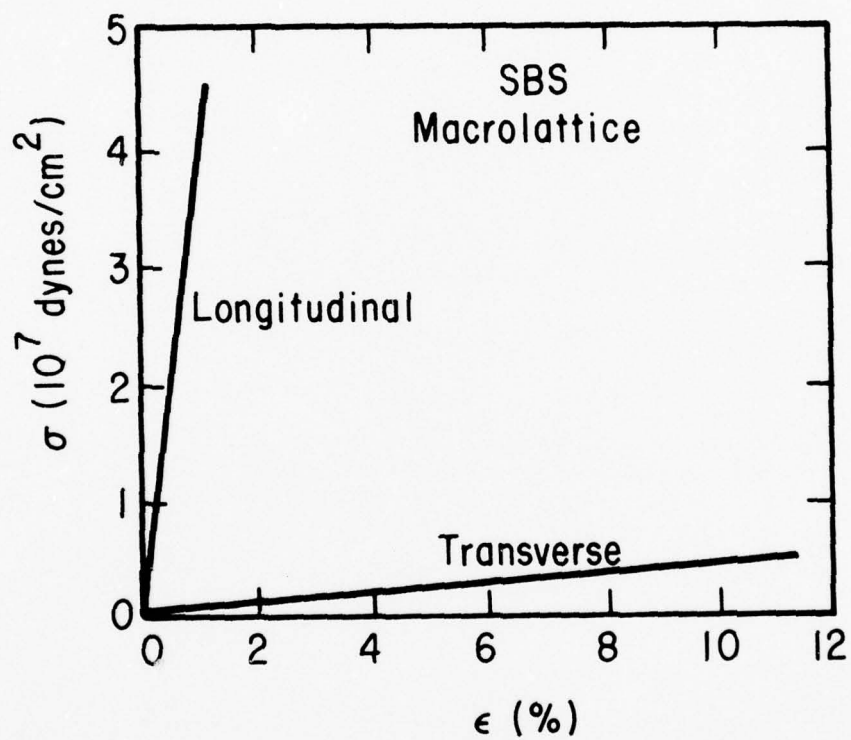
1 μ



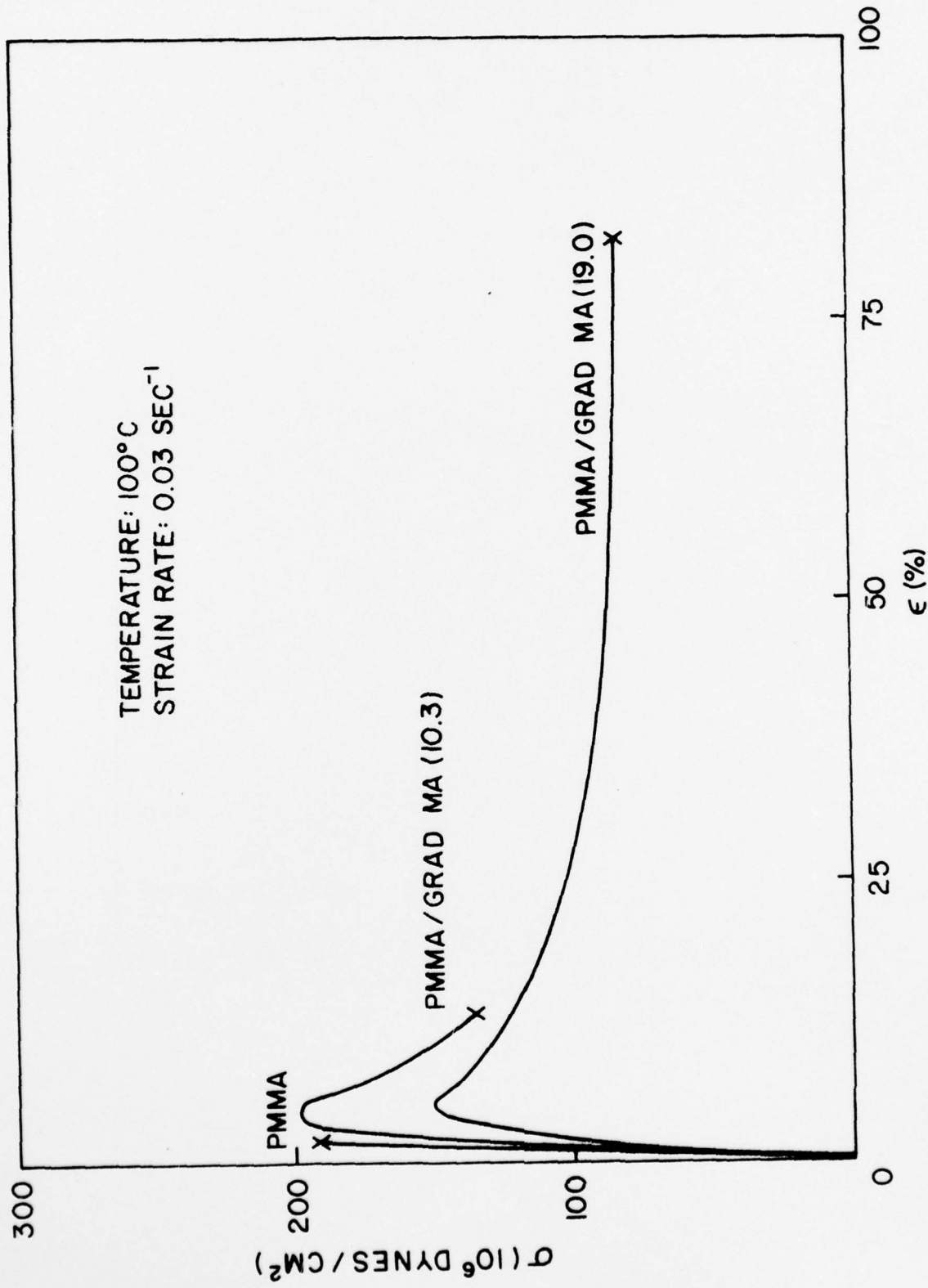






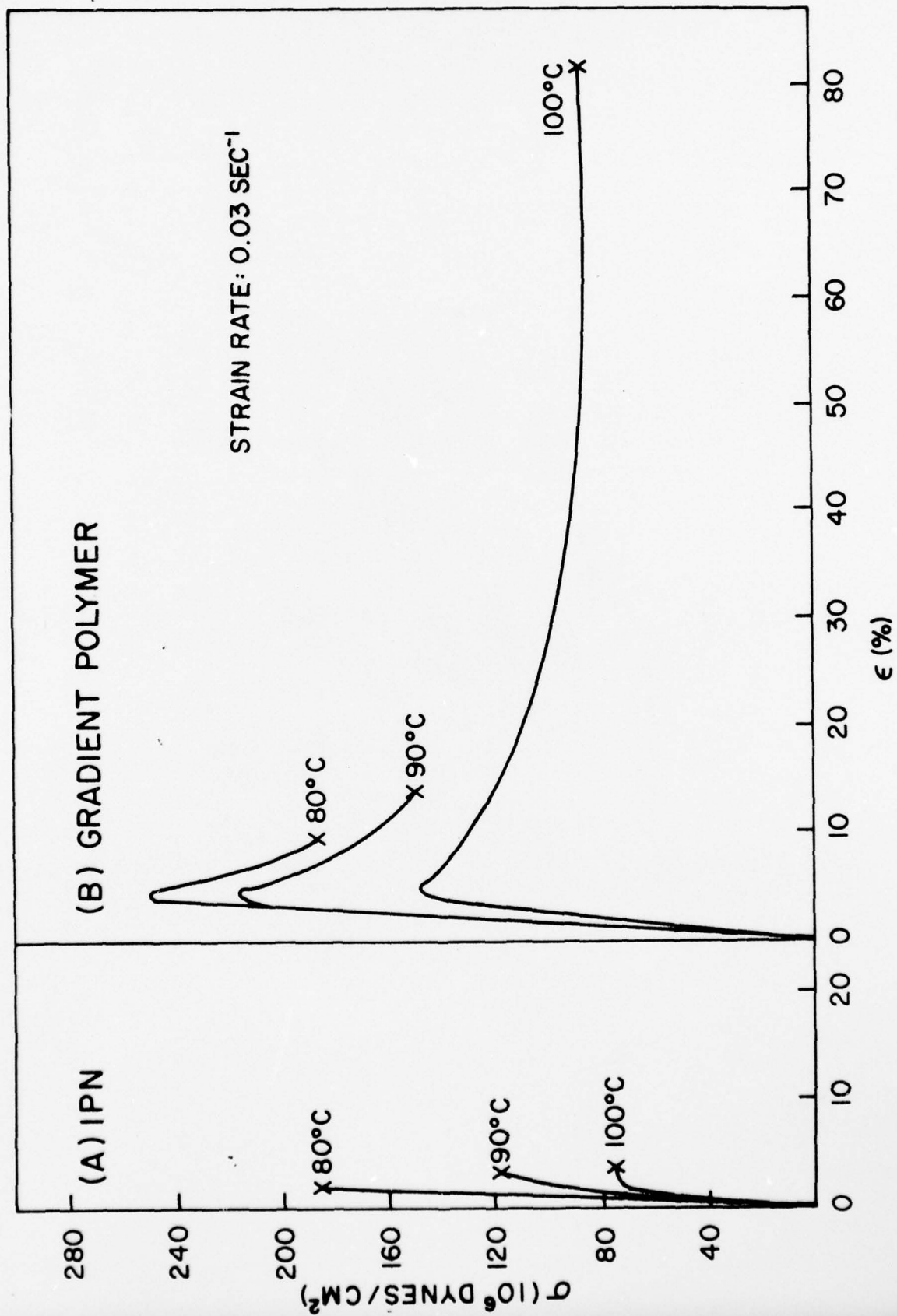


16 27 8117



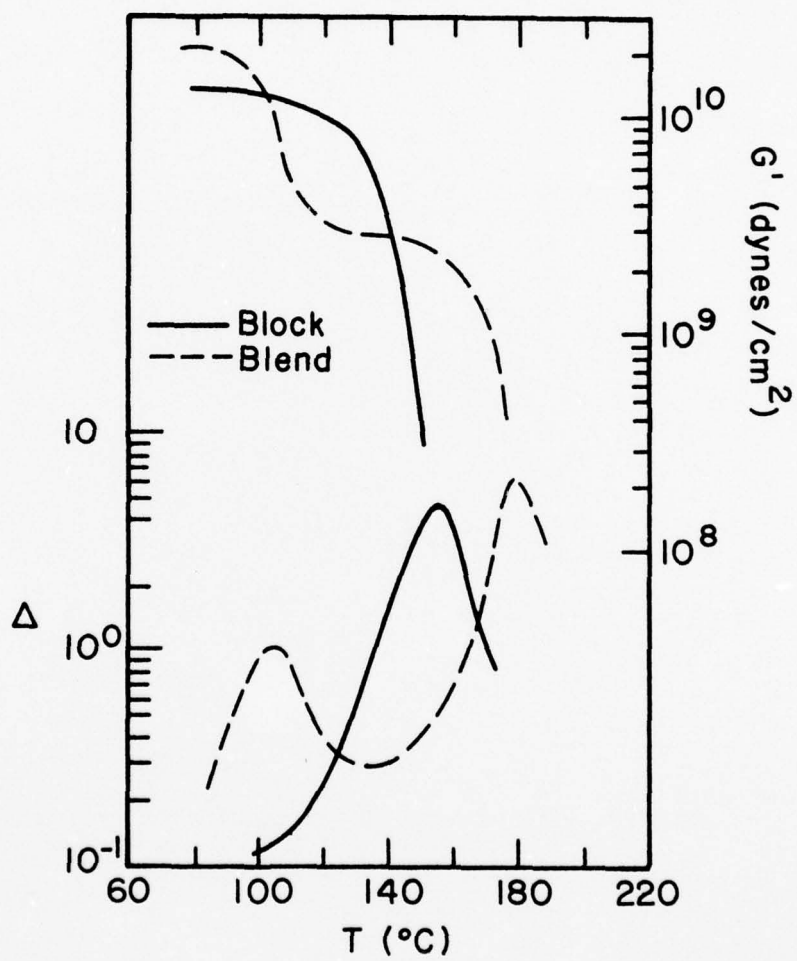
SAPS 3594 F45 87468-12

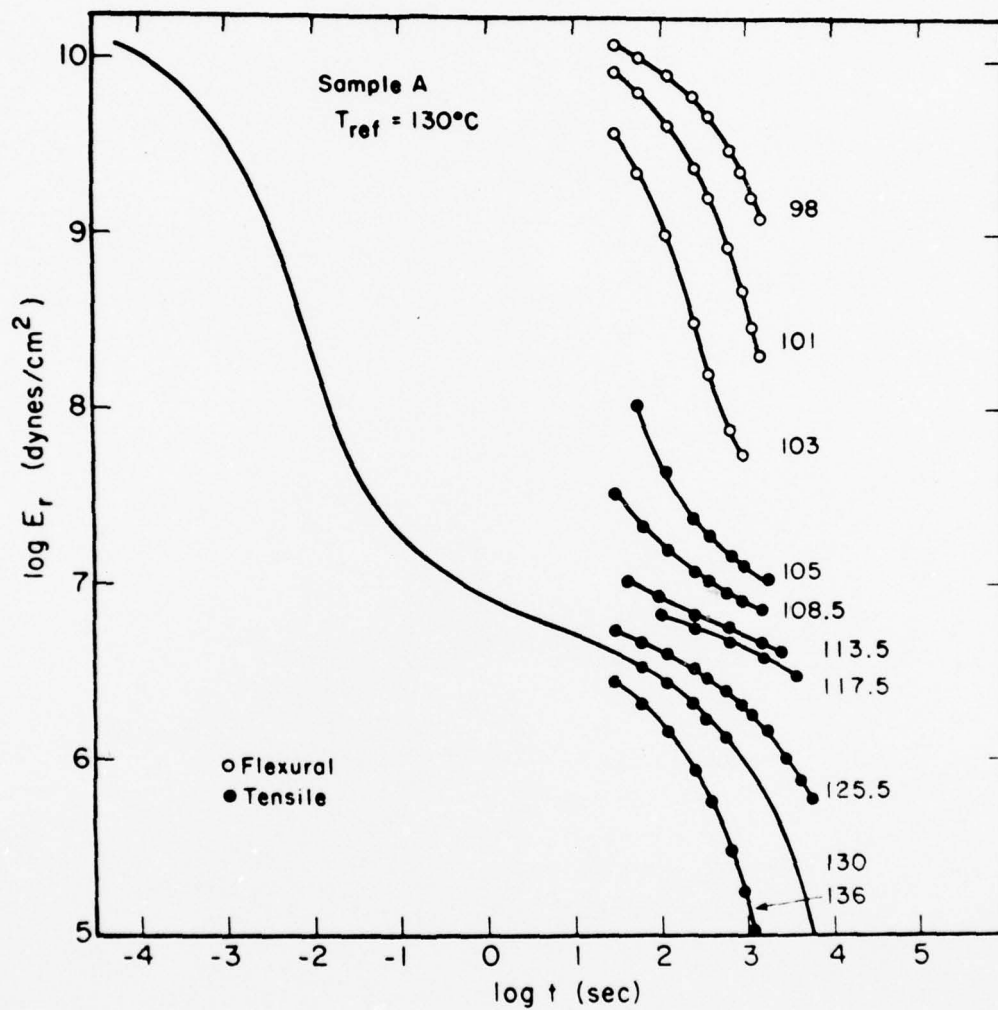
1 c 29 pica

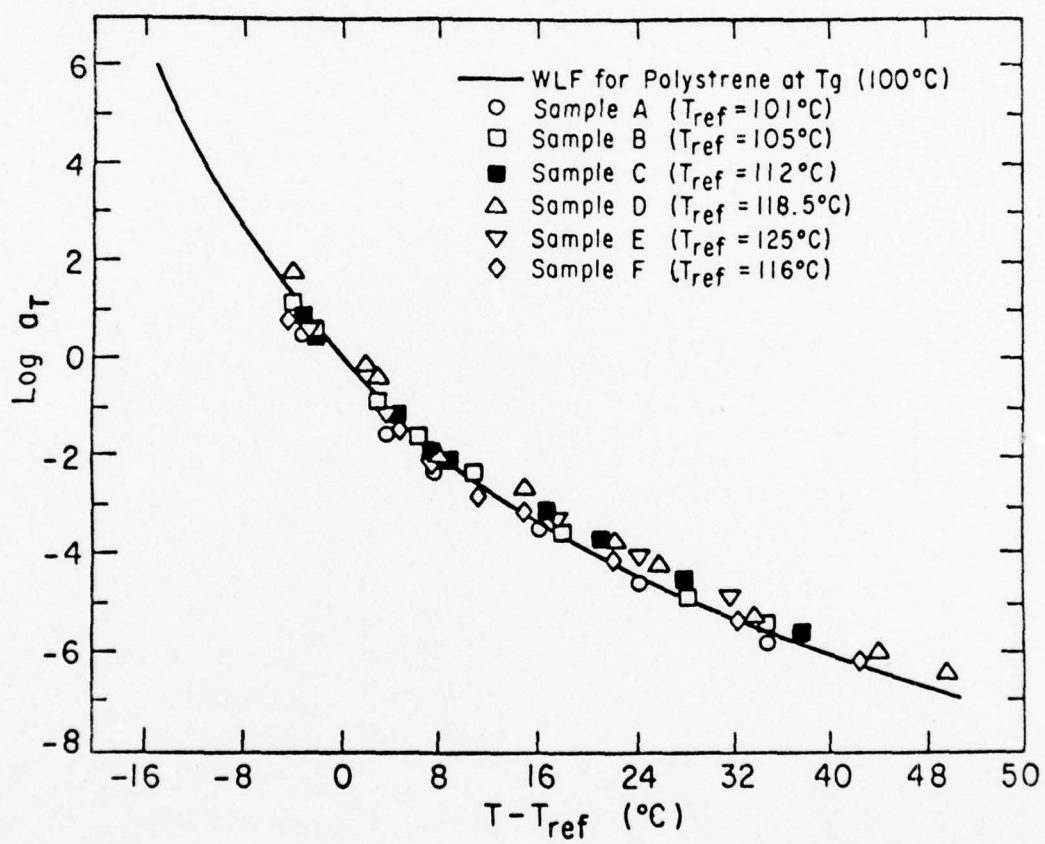


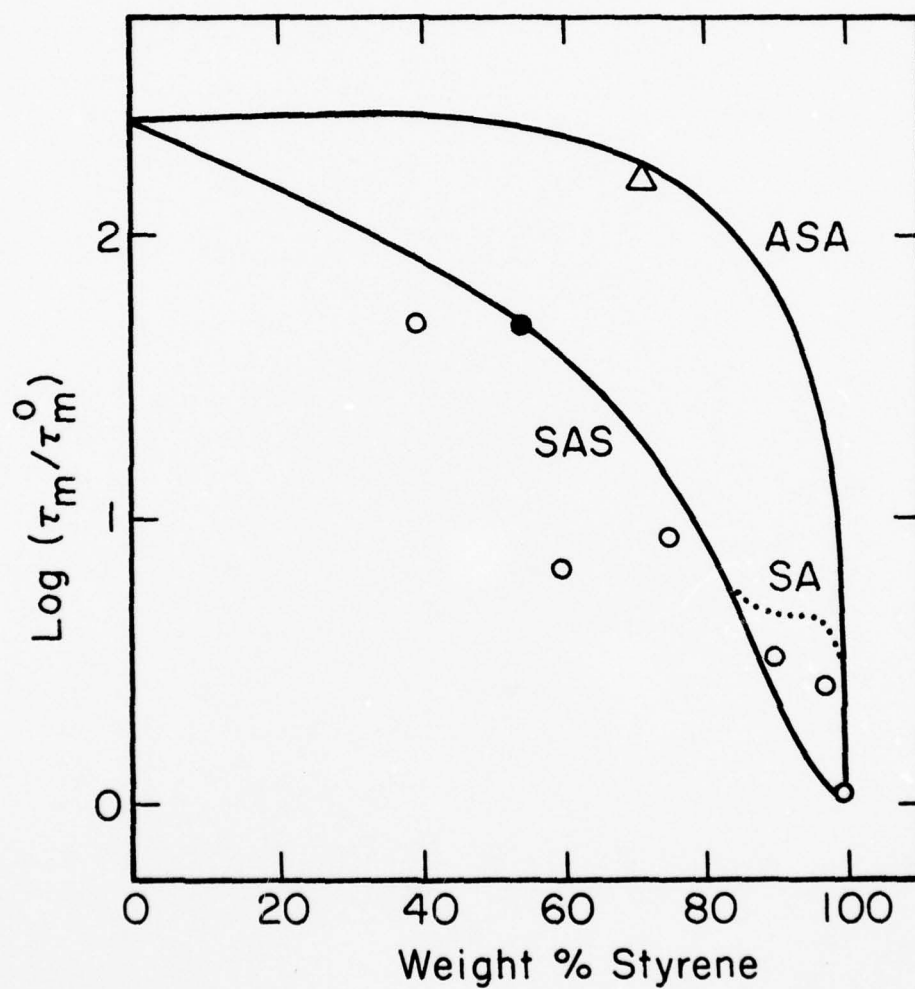
Sup 3514 F46 87418-12

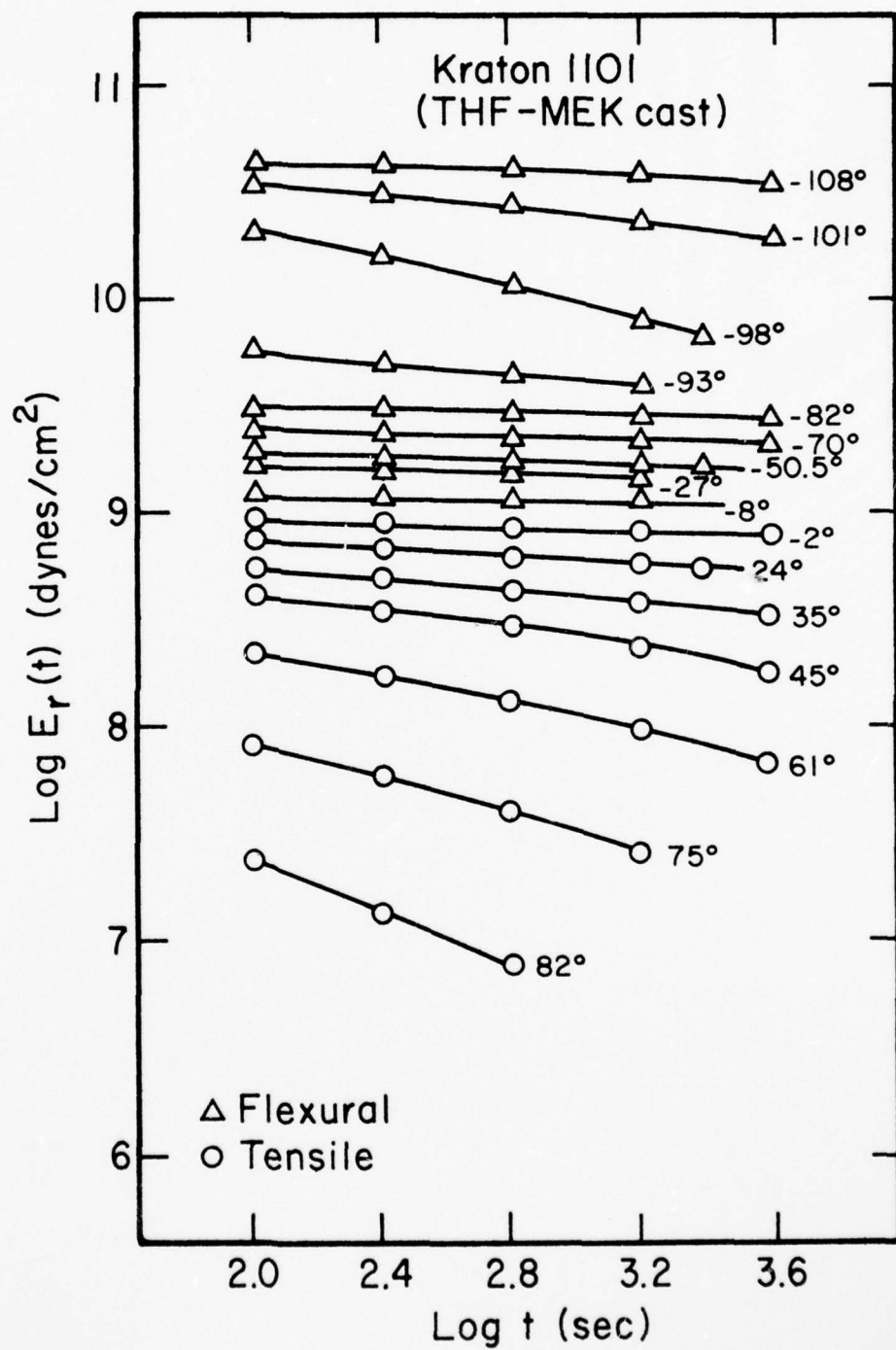
Fig 28

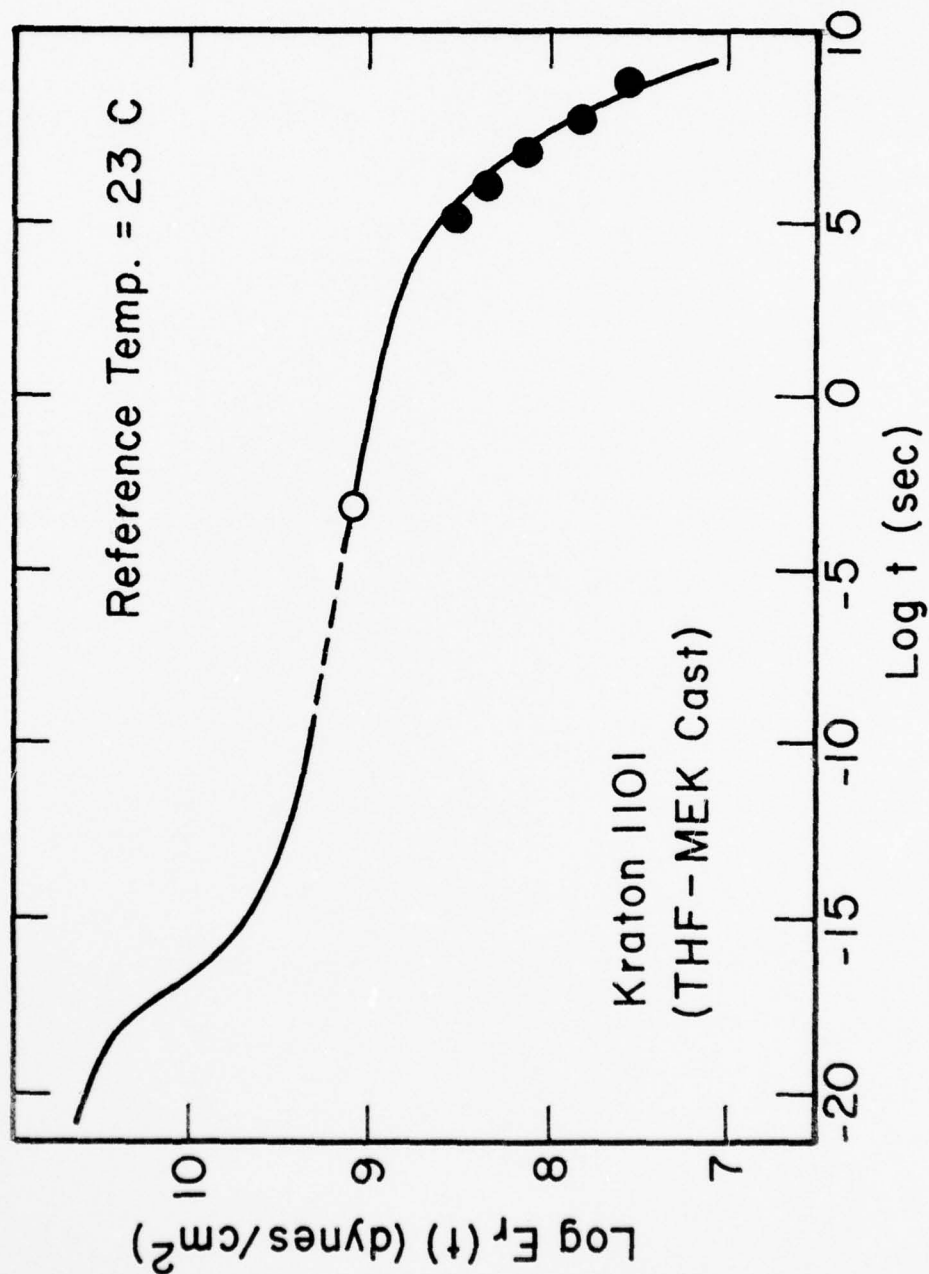












AD-A037 240

CALIFORNIA UNIV BERKELEY DEPT OF CHEMICAL ENGINEERING
PROPERTIES AND STRUCTURE OF POLYMERIC ALLOYS.(U)
FEB 77 M SHEN, H KAWAI

F/G 7/3

UNCLASSIFIED

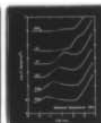
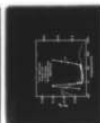
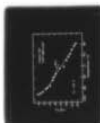
TR-11

N00014-75-C-0955

NL

2 OF 2

AD
A037240



END

DATE
FILMED

4-77

